INTRODUCING NOVEL DOUBLE POLARIZATION PEAK SHIFT SENSITIVITY (DPPSS) PARAMETER FOR ENHANCED SENSING RANGE OF LSPR SENSOR

By

Ramisha Raida Karim (180021210)

Sumaieta Tasnim (180021101)

Md. Ehsanul Haque (180021124)

A Thesis Submitted to the Academic Faculty in Partial Fulfillment for the Requirements of the Degree of

"BACHELOR OF SCIENCE IN ELECTRICAL AND ELECTRONIC ENGINEERING"

Department of Electrical and Electronic Engineering,

Islamic University of Technology (IUT)

Gazipur, Dhaka

May 2023

DECLARATION

We do, hereby declare that this project is a representation of our Thesis work as a part of the final year course work. Wherever the contribution of others is involved, every effort is made to indicate this point clearly, with due reference to literature and acknowledgement of collaborative research and discussions. The work was done under the supervision of Dr. Mohammad Rakibul Islam, Professor and Head, Electrical and Electronic Engineering (EEE) Dept. at Islamic University of Technology, Gazipur, Dhaka.

<u>Signatures of Students:</u>

Ramisha Raida Karim
Student ID: 180021210
Department: Electrical and Electronic
Engineering
Date: 29/05/2023

Sumaieta Tasnim
Student ID: 180021101
Department: Electrical and Electronic
Engineering
Date: 29/05/2023

Md. Ehsanul Haque
Student ID: 180021124
Department: Electrical and Electronic
Engineering
Date: 29/05/2023

APPROVAL

Introducing Novel Double Polarization Peak Shift Sensitivity (DPPSS) Parameter for Enhanced Sensing Range of LSPR Sensor

Students' Name and ID:

Ramisha Raida Karim (180021210)

Sumaieta Tasnim (180021101)

Md. Ehsanul Haque (180021124)

Approved By:

_____

Dr. Mohammad Rakibul Islam
Professor and Head,
Department of Electrical and Electronic Engineering,
Islamic University of Technology (IUT),
Board Bazar, Gazipur-1704.
Date: May 29, 2023

ACKNOWLEDGEMENT

In the name of Allah, we are proud to have completed our thesis work. After an intensive period of learning and developing, this note of acknowledgment is our final touch on our Undergraduate Thesis work. We would like to reflect on the people who mentored, supported, and helped us through this period. First and foremost, we would like to thank our Mentor and Supervisor Dr. Mohammad Rakibul Islam Sir, for his support, guidance and help throughout this period. Sir guided us through every step of this project during the whole period. He also provided us with the tools that were needed and helpful for the completion of the work. During times of confusion and difficulties, Sir was always available to support and guide. We are truly blessed and thankful that we were fortunate enough to do our undergraduate thesis with Sir and work under his supervision. We thank Sir deeply for his constant guidance, motivation, and help. Most importantly, we would like to thank our parents for putting their trust and faith in us, tolerating the distance, and allowing us to choose our own. We would like to thank our friends for their constant support. We also acknowledge the combined efforts of all our teammates in bringing this project to a reasonable outcome. We hope we continue to experience more learning experience together.

ABSTRACT

This research article provides a comprehensive analysis of a localized surface plasmon resonance (LSPR) based sensor, which operates in the visible to near-infrared region and uses a distinctive combination of two metals, ITO and Au as the plasmonic layers to achieve exceptional sensitivity. The wavelength spectrum this sensor can now measure has been extended by combining these two materials in the RI region of 1.30 to 1.41, allowing the sensor to function in diverse fields such as bioimaging, biosensing, photocatalysis etc. A distinct characteristic of the sensor is also discussed which is termed as double polarization peak shift sensitivity (DPPSS) indicating the detection of resonance peak shift in both x-pol and y-pol simultaneously. DPPSS is the parameter based on which efficiency of the sensor is analyzed, wavelength sensitivity (WS) and practicality of the fabrication. After optimizing all the structural parameters of the proposed sensor, it shows the highest DPPSS value of 19560 nm/RIU and the maximum wavelength sensitivity of 19630 nm/RIU. The proposed sensor shows a resolution of 5.09×10^{-6}. This indicates that the sensor can detect small changes in analyte RI, precisely in the order of 10^{-6}. The proposed parameter DPPSS shows increased range of wavelength for the detection purpose and also considers both x and y-polarizations in this regard. The advantages of using both gold and ITO has been discussed and it was observed that the sensor shows better performance with minute change detections because of the use of these two plasmonic materials. In addition to having a very high sensitivity, the suggested sensor is fabrication friendly. The proposed research serves as a foundation for a thorough exploration of the LSPR phenomena for PCF using noble metal nanospheres.

TABLE OF CONTENTS

Contents

LIST OF FIGURES

LIST OF TABLES

CHAPTER 1

INTRODUCTION

1.1 PCF Sensors

PCF stands for "Photonic Crystal Fiber," also known as "Micro structured Optical Fiber" or "Holey Fiber." It is a type of optical fiber that contains an array of microscopic airholes running along its length, forming a pattern known as a photonic crystal. PCF sensors are sensors that utilize this unique fiber structure to enable various sensing applications.

PCF sensor refers to a type of sensor technology called Polymer Capacitive Film sensor. It is commonly used in touchscreens and touch-sensitive devices to detect and respond to touch input. PCF sensors are constructed using a thin polymer film that has conductive coatings on both sides. These coatings create a capacitor, and when pressure or touch is applied to the film, the capacitance changes.

The PCF sensor operates by measuring the change in capacitance caused by the touch input. When a user touches the screen, their finger or stylus alters the electric field between the conductive layers of the sensor, resulting in a change in capacitance. This change is detected by the sensor, which then relays the information to the device's controller or processor, enabling it to interpret the touch input.

PCF sensors offer several advantages, including high accuracy, durability, and the ability to detect multi-touch gestures. They are commonly found in various devices such as smartphones, tablets, gaming consoles, ATMs, and industrial control panels. PCF sensors have contributed to the widespread adoption of touch-enabled interfaces and have become an integral part of modern touchscreen technology.
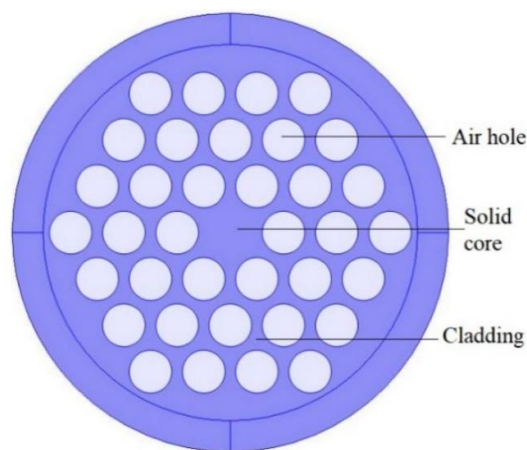
Fig 1: Photonic Crystal Fiber 1

1.2 Surface Plasmon Resonance

Surface plasmon resonance (SPR) is a phenomenon that occurs when light interacts with a thin metal film or surface, typically gold or silver, in the presence of a dielectric medium such as air or liquid. It is based on the excitation of surface plasmons, which are collective oscillations of electrons at the metal-dielectric interface.

When light of a specific wavelength, known as the resonance wavelength, is incident on the metal surface at a particular angle, the surface plasmons are excited. This results in a strong absorption of the incident light, leading to a reduction in the reflected light intensity. By monitoring the reflected light intensity as a function of the incident angle or wavelength, one can obtain information about the interactions occurring at the metal surface.

SPR is widely used in various fields, particularly in biosensing and biochemistry. In biosensing applications, biomolecules such as proteins, antibodies, or DNA are immobilized on the metal surface. When a sample containing complementary or interacting molecules is flowed over the surface, binding events occur, leading to changes in the refractive index near the metal surface. These changes can be detected as shifts in the resonance angle or wavelength, providing valuable information about the binding kinetics, affinity, and concentration of the analyte molecules.
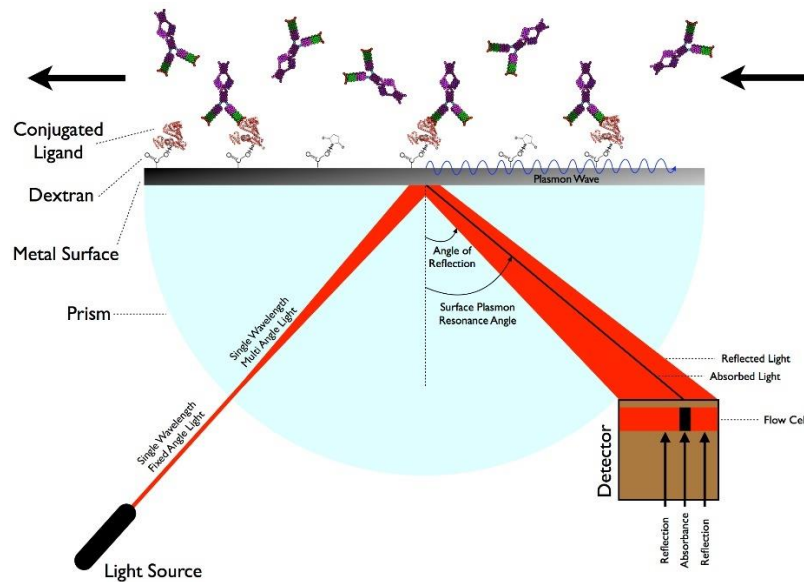
Fig 2: Surface Plasmon Resonance 1

SPR-based biosensors are label-free, meaning they do not require any fluorescent or radioactive labels, making them versatile and suitable for real-time monitoring of molecular interactions. They have applications in drug discovery, medical diagnostics, environmental monitoring, and more. Additionally, SPR techniques can also be used for studying thin films, surface chemistry, and material characterization in various scientific and industrial fields.

As technology advances, new and developed sensing systems are being introduced for practical biosensing applications. In this regard keeping the cost at low level is given a priority too. SPR is a widely used technology that has gained a great deal of recognition in the area of quantitatively analyzing the binding interactions between two biomolecules. When an incident light beam comes in contact with any metal surface at a specific angle, this phenomenon is observed. It can be observed that in the last decade, the preferred choice among designers and developers across the globe was prism coupling based SPR sensors. However, SPR sensors that are prism based were thought to have few limitations, such as inaccurate sensing applications and huge size due to additional sophisticated optomechanical elements, making them unsuitable for remote sensing.[1] The development of SPR-based PCF sensors provided a remedy for this. Thin gold film sensors are typically used in SPR, which is essential for the SPR process. Still, due to the expense and complexity of the device, most researchers cannot employ SPR technology [2]

1.3 Optical Fiber Design

Optical fiber design involves the careful engineering of the structure and materials used in the fabrication of optical fibers. Optical fibers are thin strands of flexible, transparent material that are widely used for transmitting light signals over long distances with minimal loss or degradation. Here are some key aspects of optical fiber design:

Core and Cladding: The core is the central region of the fiber through which light propagates, while the cladding is the outer layer that surrounds the core. The core has a higher refractive index compared to the cladding, ensuring that light is confined and guided along the fiber. The refractive index profile is often designed to maintain a condition called total internal reflection, which minimizes signal loss.

Mode Structure: Optical fibers can support different modes of light propagation. Single-mode fibers have a small core diameter, allowing only a single mode of light to propagate. Multimode fibers have larger core diameters, enabling multiple modes of light propagation. The choice between single-mode and multimode fibers depends on the application requirements, such as transmission distance and bandwidth.

Dispersion Management: Dispersion refers to the broadening of light pulses as they travel along the fiber. Chromatic dispersion occurs due to the dependence of the refractive index on the wavelength of light, while modal dispersion arises from the different path lengths traveled by different modes in multimode fibers. Various design techniques, such as graded-index profiles and dispersion-shifted fibers, are employed to manage and minimize dispersion effects.

Fiber Coating: Optical fibers are typically coated with a protective layer, often made of polymer materials, to provide mechanical strength, protection against environmental factors, and ease of handling during installation. The coating also acts as a buffer to prevent microbending losses that can occur when the fiber is bent.

Specialty Fibers: In addition to standard single-mode and multimode fibers, there are various specialty fibers designed for specific applications. Examples include polarization-maintaining fibers, which maintain the polarization state of light, and photonic crystal fibers, which use a periodic pattern of air holes to control light propagation characteristics.

Optical fiber design involves a combination of material selection, geometric considerations, and numerical modeling techniques to optimize the performance and characteristics of the fiber for specific applications. Advancements in fiber design have led to the development of high-speed telecommunications, fiber optic sensors, medical imaging, and other technologies that rely on efficient and reliable transmission of light signals.
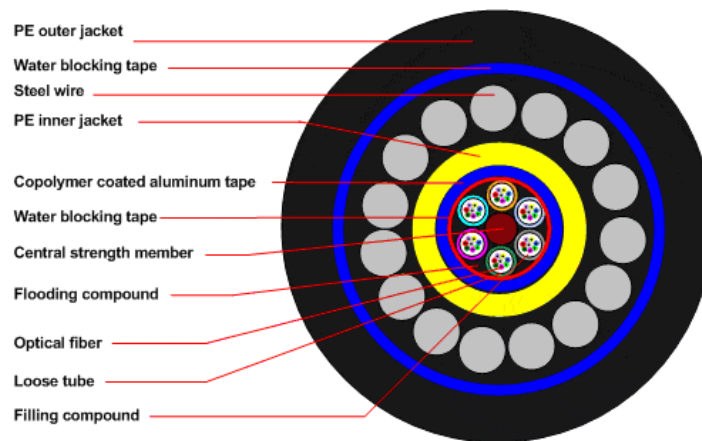
Fig 3: Optical Fiber 1

1.4 Localized Surface Plasmon Resonance (LSPR):

Localized surface plasmon resonance (LSPR) is a phenomenon that occurs when nanoparticles or nanostructures, typically metallic in nature (such as gold or silver), interact with light. Unlike surface plasmon resonance (SPR), which involves extended metal surfaces, LSPR occurs in nanoscale volumes.

In LSPR, the interaction between light and the metallic nanostructure causes the collective oscillation of conduction electrons, generating a localized electromagnetic field around the nanostructure. This localized field is highly dependent on the size, shape, and composition of the nanostructure, as well as the surrounding medium.

The LSPR phenomenon leads to unique optical properties, such as enhanced light scattering, absorption, and extinction, in the vicinity of the nanoparticles. The resonant frequency of the LSPR is determined by the characteristics of the nanostructure, including its size, shape, and composition. By tuning these parameters, the LSPR can be designed to occur at specific wavelengths in the visible or near-infrared range.

LSPR has gained significant attention in various fields, particularly in nano photonics, sensing, and biomedical applications. In sensing, the LSPR response of nanoparticles can be exploited to detect and quantify analytes in the surrounding environment. Changes in the local refractive index or the binding of molecules to the nanoparticles' surface can induce shifts in the LSPR wavelength or changes in its intensity, providing a means for label-free detection and monitoring of biomolecular interactions.

Furthermore, LSPR has applications in areas such as plasmonic sensing, imaging, photothermal therapy, catalysis, and photonics, offering unique opportunities for manipulating light-matter interactions at the nanoscale.

This is a relatively new approach which has been investigated for a longer period and is more readily available and affordable than SPR [2]It ensures that the ability to securely constrain sensing regions so that the size of any nanostructure can improve total response time, sensitivity and the throughput. Real-time observation of biomolecular binding interactions is particularly helpful. Monitoring in real-time, label-free detection, requirement of small sample size, sensor chips that are reusable, the utilization of complicated samples, and shorter experimental runs are only a few advantages it provides over other techniques [3]LSPR is produced using metal nanoparticles, often silver and gold, as opposed to traditional SPR, which employs a continuous gold sheet. In the visible light range, the LSPR generates a strong resonant absorbance peak. [1]

Only a few theoretical and experimental studies on PCF based LSPR sensors have been described, even though PCF based surface plasmon resonance have been investigated [4].

Localized Surface Plasmon Resonance (LSPR) offers several benefits in various fields and applications. Here are some of the key advantages of LSPR:

Label-Free Detection: LSPR-based sensors enable label-free detection, eliminating the need for fluorescent or radioactive labels. This simplifies the assay process, reduces costs, and avoids potential interference or alteration of the analyte due to labeling.

Sensitivity: LSPR sensors can achieve high sensitivity, allowing the detection of analytes at low concentrations. The interaction of the localized electromagnetic field with the analyte leads to changes in the refractive index, which can be detected as shifts in the resonance wavelength or

intensity. This sensitivity is particularly advantageous in applications such as biomolecular interactions, environmental monitoring, and chemical sensing.

Real-Time Monitoring: LSPR sensors enable real-time monitoring of molecular interactions or environmental changes. The response is rapid, allowing for dynamic monitoring and capturing kinetic information about binding events or changes in the analyte concentration. Real-time monitoring is valuable in fields such as drug discovery, biochemistry, and environmental analysis.

Versatile Detection Platform: LSPR sensors can be used to detect a wide range of analytes, including biomolecules, gases, chemicals, and nanoparticles. By functionalizing the sensor surface with appropriate receptors or capture molecules, LSPR sensors can be tailored to specific analytes of interest, enabling diverse applications in various fields.

Miniaturization and Integration: LSPR sensors can be designed on micro- or nanoscale platforms, enabling miniaturization and integration with other devices or systems. This allows for the development of portable, handheld, or point-of-care sensing devices with high sensitivity and specificity. The compact nature of LSPR sensors also makes them suitable for on-chip integration and high-throughput analysis.

Multiplexing Capability: LSPR sensors have the potential for multiplexed detection, enabling the simultaneous measurement of multiple analytes in a single assay. By incorporating different types of nanoparticles or nanostructures with distinct LSPR properties, or by utilizing arrays of sensors, it is possible to achieve multiplexing, thereby increasing throughput and reducing analysis time.

Compatibility with Various Sample Types: LSPR sensors can be used with a wide range of sample types, including liquid samples, gases, and complex biological matrices. This versatility allows for applications in diverse areas, such as medical diagnostics, environmental monitoring, food safety, and materials science.

These benefits make LSPR an attractive and powerful sensing technique, offering unique advantages for label-free, real-time, and sensitive detection in a variety of fields and applications.

CHAPTER 2

LITERATURE REVIEW AND METHODOLOGY

Research on plasmonic sensors has seen significant progress in recent years. Here are some notable advancements and areas of ongoing research:

Sensitivity Enhancement: Researchers have focused on enhancing the sensitivity of plasmonic sensors by optimizing the design of nanostructures, exploring new plasmonic materials, and developing novel sensing strategies. This includes engineering plasmonic resonances, utilizing hybrid plasmonic systems, and incorporating functional nanomaterials to amplify the sensing signal.

Multiplexing and Selectivity: Multiplexed plasmonic sensing, where multiple analytes can be detected simultaneously, is an active area of research. Strategies such as wavelength multiplexing, spatial multiplexing, and polarization multiplexing have been explored to achieve high-throughput and selective sensing capabilities.

Real-Time and In Situ Monitoring: Researchers are developing plasmonic sensors capable of real-time and in situ monitoring of dynamic processes. This includes studying binding kinetics, conformational changes, and molecular interactions in real-time, enabling applications in label-free biosensing, drug discovery, and environmental monitoring.

Integration with Microfluidics and Lab-on-a-Chip Systems: Plasmonic sensors are being integrated with microfluidic platforms and lab-on-a-chip systems for miniaturization, automation, and high-throughput analysis. This integration enables sample handling, analyte concentration, and multiplexed detection, leading to portable and point-of-care applications.

Biochemical and Biomedical Applications: Plasmonic sensors have found applications in various fields, including medical diagnostics, food safety, environmental monitoring, and bioimaging. Researchers are exploring the use of plasmonic sensors for early disease detection, biomarker analysis, rapid pathogen detection, and drug screening.

Theoretical Modeling and Simulation: Theoretical modeling and simulation techniques are being utilized to understand the fundamental principles of plasmonic sensing, optimize sensor

designs, and predict sensor performance. These tools help guide experimental efforts and provide insights into the underlying physics of plasmonic.

Overall, the progress of research on plasmonic sensors has led to improved sensitivity, selectivity, and functionality, expanding their applicability in various fields. Ongoing efforts continue to push the boundaries of plasmonic sensing, with a focus on advancing the fundamental understanding, technological development, and practical implementation of these sensors.

2.1 Objective

Research on Localized Surface Plasmon Resonance (LSPR) sensors aims to achieve several objectives to enhance their performance, broaden their applications, and improve their overall efficiency. Some of the key objectives of research on LSPR sensors include:

Sensitivity Enhancement: Researchers aim to improve the sensitivity of LSPR sensors to detect and quantify analytes at lower concentrations. This involves optimizing the design of plasmonic nanostructures, such as nanoparticles or nanoholes, to enhance the interaction between the analyte and the localized surface plasmons.

Selectivity and Specificity Improvement: Enhancing the selectivity and specificity of LSPR sensors is crucial to minimize false-positive or false-negative results. Researchers investigate various functionalization techniques to modify the surface of plasmonic nanostructures and selectively capture target analytes while reducing non-specific interactions.

Multiplexing Capabilities: Multiplexing refers to the ability to simultaneously detect and distinguish multiple analytes using a single LSPR sensor platform. Researchers aim to develop strategies and techniques to achieve multiplexed detection, enabling the simultaneous analysis of multiple targets in complex samples.

Real-Time and Label-Free Monitoring: One of the advantages of LSPR sensors is their capability for real-time and label-free monitoring of biomolecular interactions. Research focuses on improving the temporal resolution of LSPR sensors to capture dynamic binding events and enabling real-time analysis without the need for additional labeling or detection reagents.

Miniaturization and Integration: Researchers aim to miniaturize LSPR sensor devices, making them more portable, cost-effective, and suitable for point-of-care applications. Integration with microfluidic systems, electronics, and data analysis tools is also a research objective to create compact and user-friendly LSPR sensing platforms.

Compatibility with Complex Matrices: LSPR sensors are often employed for the analysis of complex samples, such as biological fluids or environmental samples. Research focuses on developing strategies to mitigate interference and enhance the robustness of LSPR sensors when working with complex matrices, improving their accuracy and reliability.

Novel Materials and Architectures: Exploring new materials and innovative architectures for plasmonic nanostructures is an ongoing objective. Researchers investigate alternative materials with improved plasmonic properties, such as transition metal nitrides or graphene, and novel structures like nanorods, nanoshells, or hybrid nanostructures, to enhance the performance of LSPR sensors.

By addressing these objectives, research on LSPR sensors aims to advance their capabilities and pave the way for their broader adoption in various fields, including bioanalytical research, medical diagnostics, environmental monitoring, and food safety analysis, among others

2.2 Literature Review

Over the years different metals and combinations of different elements were used for observing the performance of the LSPR based sensors in terms of amplitude sensitivity (AS), wavelength sensitivity (WS), FOM, FWHM, Birefringence's sensitivity etc. Rakibul Islam et al proposed a double peak SPR-PCF sensor with the maximum WS of 43600 nm/RIU and a maximum AS of 4602.67 nm/RIU for wavelength sensing range of 1.27 – 1.45 um. Md. Asaduzzaman Jabin et al. suggested a Titanium coated SPR based PCF sensor which is D shaped having a maximum [5]AS and WS of -360 RIU-1 and 18550 nm/RIU respectively for hemoglobin sensing. In most cases, gold has been successfully proven to be the most suitable material in achieving higher sensitivity because it is chemically stable, has no problem of oxidation and sensitive to small changes in RI. ITO (Indium Tin Oxide) is a material that has been used as coatings in SPR sensors which eventually proved to be a resourceful material in terms of performance. According to Chao Liu et al use of ITO coatings in SPR infrared sensor resulted in obtaining a

maximum AS of 442.47 RIU-1 and maximum WS of 2000-15000 nm/RIU for wavelength ranging from 1200-2250 nm [6]

By altering preparation condition, material properties of ITO can be systematically tuned. Moreover, ITO is a better conductor, comparatively cheaper than gold and silver, shows a lower loss in the infrared wavelength range and is more convenient due to adjustable photo-electric properties [7]. As a result, a dual core model having Gold and ITO as coating material in plasmonic layers which can have operations in wide range of wavelength in both the x polarization and y polarization has been proposed to analyze the sensing parameters. Use of two metals in SPR sensors is a common phenomenon for its visible advantages. In many cases bimetallic layer increased sensitivity, resolution enhancement, increased signal to noise ratio of SPR devices, operated in wide range of RI and wavelength and also prevented the problems of one material as an outer layer [8]

According to Bhishma Karki et. Al, the use of Au/BaTiO3/BP, Ag/BaTiO3/BP and Cu/BaTiO3/BP structured sensors obtained sensitivities 0.55, 1.5 and 1.86 folds greater than that of the use of only gold (Au), silver (Ag) and copper (Cu) based sensors. Besides, detection of unknown analyte in multirange of RI open doors of opportunities in various fields including pharmaceutical sectors, bio sensing etc. In comparison to SPR, more unique properties like higher sensitivities and higher figure of merit (FOM) are obtained from LSPR based sensors [9]

Previous analysis on LSPR based sensors showing maximum WS of 46300 nm/RIU and maximum AS of 8485.2 RIU-1 were done using AZO and gold as two plasmonic layers simultaneously [10]Again, a combination of plasmonic layers with materials Titanium Di oxide and gold obtained of 3616 RIU-1 and 12000nm/RIU as maximum amplitude and wavelength sensitivity respectively [5]

[11]and [12]describe a PCF-based sensor for detecting blood components. The authors of [11]examined the sensitivity analysis for RBC, hemoglobin, WBC, plasma, and water, however their sensitivity for all analytes was inadequate. The achieved confinement losses were likewise inadequate. The authors presented a crystalline core PCF for sensing several blood components in [12]For RBC, hemoglobin, WBC, plasma, and water, they attained sensitivity of 80.9%, 80.6%, 80.1%, 79.9%, and 79.4%, respectively. For the same analytes, they measured confinement loss of 1.21013 dB/cm, 8.61014 dB/cm, 4.91014 dB/cm, 2.91014 dB/cm, and 1.11014 dB/cm. They have significantly increased sensitivity and confinement loss, but there is

still room for improvement. In this article, various types of blood components such as RBC, hemoglobin, WBC, plasma, and water will be evaluated using various instruments to validate the sensor's quality. [13]

An octagonal shaped hollow core PCF with eight head star cladding is created and examined in this work for different important optical features of cholesterol sensing in liquid samples. The investigated result of the proposed sensor yields a very high sensitivity profile of 98.75% at 2.2 THz. Furthermore, the proposed PCF yielded a very small confinement loss of 3.14 10-20 and a very low effective material loss of 0.0008 cm^{-1} in the instance of cholesterol detection. This analysis has also revealed a relatively flat dispersion profile of 0.31 ps/THz/cm. The practicality of fabricating the designed PCF on the existing fabrication platform demonstrated its appropriateness for practical implementation, and it will make a significant contribution to chemical and other bio-sensing applications. [14]

In the research work stated in [15], a unique structure with a hexagonal symmetrical covering and a hollow core is being investigated, which promises to play a significant role in the field of sensing applications. The investigation spans a frequency range of 2 THz (1-3 THz). Zeonex was employed as the background material, and the findings show that in ideal conditions, the sensitivity for benzene, water, and methanol is 99.76%, 99.44%, and 99.39%, respectively.

There are several works exhibited based on different shapes as well. For example – one of the investigations reveals that the suggested model has a 99.98% sensitivity and a relatively low confinement loss of 4.7210^{-22} cm^{-1} for tryptophan, the rarest of the essential amino acids found in proteins. The cladding's superior sensing capabilities are obtained by incorporating two hollow square air cavities encircled by four rectangular air channels [16]. In another suggested sensor, in the spectrum of 1.35-1.41 for the analyte refractive index (RI), the proposed sensor achieves a maximum wavelength sensitivity of 14,500 nm / RIU in X-polarization mode and a maximum amplitude sensitivity of 4738.9 RIU^{-1} in Y-polarization mode. This sensor offers the lowest wavelength sensor resolution of 6.910^{-6} RIU and the lowest amplitude sensor resolution of 2.1110^{-6} RIU for Y-polarized mode, with FOM of 387 and 364 for X and Y polarization, respectively [17].

Another suggested sensor of gold shows maximum amplitude sensitivity and wavelength sensitivity (WS) in x-polarization mode as 1757.3RIU^{-1} (Refractive Index Unit) and 32,000 nm/RIU, respectively. Furthermore, the proposed design has a high sensor resolution of

1.42810^{-6} and a figure of merit of 587.2, indicating a high-performance sensor, as well as birefringence of 0.004 RIU [18]. Again, a wheel-structured Zeonex-based hexagonal packing photonic crystal fiber (PCF) sensor with a refractive index of 1.3423 and a refractive index of 1.3459 has been proposed for sensing camel milk. Within a terahertz (THz) range of 0.2 to 2.0 THz, this sensor was studied for porosities of 85%, 90%, and 98%. This sensor has a maximum sensitivity of 81.16% and 81.32% for camel and cow milk, respectively, at an operating frequency of 2 THz. At the same operating conditions, camel milk had an EML of 0.033013 cm^{-1} and cow milk had an EML of 0.03284 cm1 with negligible confinement losses of 8.675×10^{-18} cm^{-1} 1.435 ×10^{-18} cm^{-1}[19]

a basic circular-shaped plasmonic biosensor based on photonic crystal fiber for identifying several blood components in the near-infrared and visible spectrums was proposed which had higher amplitude sensitivity of 5078.99 RIU^{-1}, maximum resolution of 5.13× 10^{-5} and an overall excellent FOM trait of 325 in the HEy11 mode. For HEx11 mode, the corresponding values are 2576.38 RIU^{-1}, 5.71× 10^{-5}, 250, respectively [20].

Another eye shaped LSPR showed the maximum wavelength sensitivity of 14,000 nm/RIU (refractive index unit) with a sensor resolution of 7.14×10^{-6} RIU. Also, the maximum amplitude sensitivity is reported to be 4779.7 RIU^{-1}. The measurement took place inside the 1.33–1.41 index of refraction range [21]. The research in [22]shows that because of the careful placement of the circular air holes with silica as the fiber material, which is surrounded by successive layers of TiO2 and gold (Au), the sensor performance has substantially increased. The TiO2 layer improves sensitivity while also increasing the adhesiveness of Au on the fiber. It shows maximum amplitude sensitivity of 3807 RIU−1, the maximum wavelength sensitivity of 80,500 nm/RIU, the maximum sensor resolution (wavelength) of 1.24× 10^{-6} RIU, and the maximum sensor resolution (amplitude) of 2.63×10^{-6} RIU, and the maximum figure of merit (FOM) was found to be 2115. Researchers have been working on optimizing the performance characteristics of PCF sensors, such as sensitivity, resolution, and response time. This involves exploring new materials with improved dielectric properties, developing advanced fabrication techniques, and optimizing the sensor's structural design. Another suggested PCF has an ultra-low effective material loss of 0.013 cm1 and 0.020 cm1 in x and y polarization modes, respectively, with a fattened dispersion of 0.020 ps/THz/cm and 0.065 ps/THz/cm at 1 THz. Furthermore, the proposed PCF structure is being researched for sensing various liquid compounds (cholesterol, methanol, ethanol, and benzene) and air pollutants (cyanide, dioxin,

nitrogen oxide, and hydrogen sulfide). It is demonstrated that the proposed PCF outperforms several recently published designs in the literature. [23]

A simple, fabrication-friendly, extremely low loss photonic crystal fiber sensor based on surface plasmon resonance was also observed. A di-material plasmonic layer of 20 nm Gold (Au) and 10 nm Titanium Dioxide (TiO2) is used in our proposed sensor. The Finite Element Method of COMSOL Multiphysics (v. 5.5) was used to identify variations in the sensor's optical characteristics. After optimizing all cross-sectional parameters, the sensor model achieved maximum Amplitude Sensitivity and Wavelength Sensitivity of 4646.1 RIU^{-1} and 10,000 nm/RIU with sensor resolutions of 2.15×10^{-6} RIU and 1.00 10-5 RIU within the 1.33-1.42 RI range for analyte sensing. Furthermore, good sensitivities were established for strain, temperature, and magnetic field strength (MFS) sensing, with maximum values of 4.0 pm/ (0.004 nm/), 1.00 nm/°C, and 160 pm/Oe (0.16 nm/Oe), respectively. The proposed sensor performed admirably in sensing minute changes in analyte RI, strain, temperature, and MFS, making it a one-of-a-kind and significant addition to the scientific, biomedical, and industrial areas [24].

Some arrays of gold and aluminum-doped zinc oxide (AZO) use plasmonic materials to create a unique photonic crystal fiber sensor with various loss peaks. A novel dispersion relation with several peaks has been established using plasmonic layer arrays. In comparison to a single-peak sensor, the suggested sensor includes numerous peaks that can be used for diverse wavelength ranges to detect the refractive index efficiently. This publication proposes a new interrogation approach called Peak Amplitude Difference Sensitivity (PADS), whereas this sensor achieves a maximum PADS of 396.175 RIU 1 and a maximum wavelength sensitivity (WS) of 85,300 nm/RIU. The sensor also offers a high wavelength resolution of 1.17 10 6 RIU. With R2 = 0.99978, the linearity is extremely high. Some arrays of gold and aluminum-doped zinc oxide (AZO) use plasmonic materials to create a unique photonic crystal fiber sensor with various loss peaks. A novel dispersion relation with several peaks has been established using plasmonic layer arrays. In comparison to a single-peak sensor, the suggested sensor includes numerous peaks that can be used for diverse wavelength ranges to detect the refractive index efficiently. This publication proposes a new interrogation approach called Peak Amplitude Difference Sensitivity (PADS), whereas this sensor achieves a maximum PADS of 396.175 RIU^{-1} and a maximum wavelength sensitivity (WS) of 85,300 nm/RIU. The sensor also offers a high

wavelength resolution of 1.17×10^{-6} RIU. With R2 = 0.99978, the linearity is extremely high [25].

The glass surface is covered with a small layer of TiO2, which attracts the field from the core guided mode and helps the gold (Au) adhere to the fiber. As a result of the dielectric refractive index (RI) shift from 1.33 to 1.41, simulation results using geometric parameters show a maximum wavelength sensitivity of 16,000 nm/RIU (Refractive Index Unit) for x-polarization and 17,000 nm/RIU for y-polarization, respectively. It is demonstrated that the suggested sensor's greatest achieved amplitude sensitivity is 4596 RIU^{-1} and 4557 RIU^{-1} for x-polarization and y-polarization, respectively, with maximum losses of 3.73 dB/cm and 4.48 dB/cm. Additionally, the highest birefringence of 8.8984×10^{-4}, the maximum sensor resolutions (amplitude) of 2.18×10^{-6} and 2.19×10^{-6}, the maximum sensor resolutions (wavelength) of 6.25×10^{-6} and 5.88×10^{-6} for the x- and y-polarization modes, respectively, are achieved. The aforementioned sensor is anticipated to help to the precise detection of biological and organic chemical analytes because of its excellent detecting properties [26].

A Surface Plasmon Resonance-based Photonic Crystal Fiber (SPR-PCF) sensor with an extremely high sensitivity that can sense analyte, temperature, and magnetic field simultaneously. The prototype is easily fabricable using the common Stack-and-Draw technique and contains a trigonal cluster-based strategic layout of circular air holes inside the fiber. The plasmonic materials utilized to surround the PCF are composed of very thin layers of titanium dioxide (TiO2) and gold (Au). The sensor properties are calculated using the Finite Element Method (FEM) of the commercial program COMSOL Multiphysics 5.3a. A maximum amplitude sensitivity (AS) of 7223.62 RIU^{-1}, a maximum wavelength sensitivity (WS) of 28,500 nm/ RIU, and a leading figure of merit (FOM) of 914 RIU^{-1} after optimizing various parameters was observed. With sensor resolutions of 1.38×10^{-6} (amplitude) and 3.51×10^{-6} RIU (wavelength), the sensor may identify unidentified analytes in the refractive index (RI) range of 1.33 to 1.42. It can also detect changes in temperature and magnetic field with maximum sensitivity of 1.25 nm/C (1250 pm/C) and 0.16 nm/Oe (160 pm/Oe), respectively. For the 10% manufacturing tolerance analysis, a minute variation in the sensor's performance was seen. We can therefore draw the conclusion that our sensor, with its exceptional sensing capabilities and flexible features, can considerably advance the domains of science, biomedicine, and industry [27].

Al-doped ZnO was also used to serve as a plasmonic material to boost sensor performance and allow for flexible design. The entire numerical investigation uses the finite element approach. Investigations on resonance quality, sensitivity, sensor resolution, sensor length, and figure of merit (FOM) have been sparked by observations made using the best conditions. The proposed structure has a greater amplitude sensitivity of 5078.99 RIU^{-1}, a maximum resolution of 5.13×10^{-5}, and an overall excellent FOM trait of 325 in the HEy11 mode, according to numerical studies. The comparable numbers for HEx 11 mode are 2576.38 RIU^{-1}, 5.71× 10^{-5}, and 250, respectively [20].

Prism-based SPR sensors were thought to have some limitations, such as inaccurate sensing applications and bulky size due to additional sophisticated optomechanical elements, making them unsuitable for remote sensing [28]. A maximum amplitude sensitivity (AS) and wavelength sensitivity (WS) of 5060 RIU^{-1} and 41500 nm/RIU, respectively, after optimizing all of the fiber parameters was obtained in research. The maximum sensor resolution was 2.41×10^{-6} for wavelength and 1.98×10^{-6} for amplitude. Additionally, the highest figure of merit (FOM) obtained was 1068.7, and the highest amount of birefringence was discovered to be 1.568×10^{-3}. The sensor has a fabrication tolerance limit of 10% and an overall analyte sensing range of refractive indices 1.32 to 1.43. Additionally, our sensor has a resolution (temperature) of 1.33×10^{-1} C and estimated sensitivities to temperature and strain of 0.75 nm/C and 3 pm/C, respectively [29].

The two modes (core and plasmonic) can be excited by using gold (Au) or AZO (aluminum-doped zinc oxide). When gold was used as the plasmonic material, simulation results showed very high amplitude sensitivity (AS) of 4358.09 RIU^{-1}, maximum wavelength sensitivity (WS) of 21,000 nm/RIU, a high figure of merits (FOM) of 729, and sensor resolutions of 4.76×10^{-6} RIU^{-1} and 2.29×10^{-6} RIU^{-1} for wavelength and amplitude, respectively. The equivalent values for gold replaced with AZO were 3908 RIU^{-1}, 1700 nm/RIU, 792, 5.88 105 RIU, and 2.56×10^{-6} RIU^{-1}. The range of the analyte refractive index (RI) for AZO is 1.31–1.39 and for gold it is 1.33–1.42 [30]. Prism-based SPR sensors have some limitations, such as being large and having remote sensing, despite being more affordable and widely available. [31]

The sensor's in-depth analysis and numerical simulation show that it has an optimal wavelength sensitivity, specifically for X polarization, of about 14,500 nm/ RIU, a maximum amplitude sensitivity of 4738.9 RIU, and a minimum amplitude sensor resolution of 2.11 10 6 RIU for Y

polarization mode, respectively, in the range of 1.35 to 1.41 for the analyte refractive index (RI). For x and y polarization, FOM values of 387 and 364 are achieved, respectively [17].

Biosensors are analytical tools that combine chemical detectors and biological components. Comparing biosensors based on surface plasmon resonance (SPR) to other sensing technologies, such as PCF sensors, fiber Bragg grating (FBG) sensors, photoluminescence, micro-ring resonators, and resonant mirrors, surface plasmon resonance (SPR) sensors have undergone extensive development and implementation [28], [32]–[35].

In another research, a straightforward single-layer square lattice plasmonic PCF biosensor with external sensing operability is suggested. The goal of this research is to present a draft that is entirely based on annular air holes [18].

AIn research work [22], good sensitivity performance dual cluster and dual array-based PCF-SPR biosensor is described. To achieve high amplitude sensitivity, every structural factor, including the diameter of each circle, the gold and TiO2 layer thickness, and the analyte layer thickness have been turned. To direct the EM wave towards the surface and improve the sensing performance, air holes are purposefully positioned inside the fiber. Using amplitude and wavelength interrogation methods, the results showed that the numerical values of amplitude sensitivity (AS), wavelength sensitivity (WS), sensor resolution (wavelength), sensor resolution (amplitude), and FOM were 3807 RIU^{-1}, 80,500 nm/RIU, 1.24×10^{-6} RIU^{-1}, 2.63×10^{-6} RIU^{-1}, and 2115, respectively [36].

Surface plasmon resonance (SPR) based biosensors have had a noticeable effect over the past two decades in a variety of real-world applications. These empirical applications cover crucial areas like water testing, sensing of organic compounds, and gas detection as well as activities like identifying various viruses, protecting food quality, environmental monitoring, medical diagnostics, temperature sensing, strain sensing, and environmental monitoring [37]–[46].

Terahertz sensors, PCF sensors, and fiber Bragg grating have all been thoroughly studied, but SPR sensors are more prominent because of their adaptability in design, high sensitivity, and accuracy in the diagnosis of unidentified analytes [47]–[52]

The PCF, however, has been demonstrated to be superior than normal optical fiber because of its intriguing characteristics, including high confinement, single-mode of propagation, controlled birefringence, design flexibility, compact size, airborne propagation, and solid core [53]–[59].

In another research, a twin spider-shaped SPR-PCF sensor with gold coating and a small layer of TiO2 for improved gold adhesion is presented. External sensing for the y polarization mode is the sensing strategy employed here [60]. Surface plasmon waves (SPW) are the result of the evanescent field's and the free electrons' inherent frequency matching.[61]

Remote sensing can be done with fiber-based sensors. A better version of the sensor is created after much research and is known as a photonic crystal fiber (PCF)-based SPR sensor. In comparison to other fiber-based sensors, it can offer higher sensitivity and a smaller resonant peak [15], [34], [47], [51], [56], [62]. In research, [63]order for the resonance effect to be noticeably amplified by the evanescent waves, a straightforward circular lattice structure with a delicate layer of gold as the plasmonic material maintains the external sensing in a preferred fashion. To improve the adhesion of gold on fiber, a coating of TiO2 was added. The two modes (core and plasmonic) can be excited by using gold (Au) or AZO (aluminum-doped zinc oxide) [30]. SPR technology also enables the combination of nano-electronic and nano-photonic components to produce ultra-compact optoelectronic devices [64], [65].

Many of these suggested sensors either exhibit low sensitivity or are extremely challenging to manufacture for real-time applications. In a research work, [18]a straightforward, easily fabricated PCF SPR sensor with a circular form that exhibits great sensitivity in the visible and near-infrared spectra was proposed. For the purpose of sensing liquid analytes at the THz frequency range, a sectored circular porous core PCF is proposed in research work [66]

Besides all these, numerous studies have shown highly sensitive PCF-based sensors for the detection of liquid and chemical analytes in the literature [52], [56], [67]–[74].

In order to distinguish between various blood elements based on the refractive index in the THz spectrum, a PCF geometry has been presented. At the chosen operating frequency of 4.5 THz and under ideal geometric conditions, the maximum sensitivity values that have been attained are 99.18% for RBCs, 99.02% for hemoglobin, 98.81% for WBCs, 98.68% for plasma, and 98.35% for water [75]. For sensing purposes, a hollow core design resembling a spider web was suggested. At 4.5 THz, the proposed device showed a sensitivity of 99.99% and a very low EML of 0.000263 cm^{-1} [76].

2.3 Methodology

The determination of different parameters was done using COMSOL Multiphysics. At first the geometry was constructed in the software and then meshing was done. The different plasmonic

layers were put and then necessary parameters were given as input. After that, simulation was done varying the parameters like refractive index. The sensitivity calculation along with other parameters like- bi refringence, resolution, Double Polarization Peak Shift Sensitivity (DPPSS) etc. were done using necessary equations.

To calculate the sensitivity of a PCF (Polymer Capacitive Film) sensor using COMSOL, we followed these general steps:

Geometry and Material Setup: A first the geometry of the PCF sensor in the COMSOL environment, defining the dimensions and structure of the sensor was created. Appropriate material properties to the different components of the sensor, including the polymer film and conductive coatings were assigned.

Physics Settings: The physics involved in the PCF sensor operation was defined. This typically includes the electrostatics module for capacitance calculations. Appropriate boundary conditions, such as electrode potentials or charge densities were specified.

Meshing: A mesh for the sensor geometry to discretize the computational domain was generated. The mesh was fine enough to capture the details of the sensor structure and any variations in the electric field.

Solver Configuration: A suitable solver and configure the solver settings based on the specific problem was considered. The desired level of accuracy, computational resources, and convergence criteria was found.

Sensitivity Calculation: Once the simulation setup is complete, we proceeded to calculate the sensitivity of the PCF sensor. Sensitivity is typically defined as the change in capacitance with respect to the quantity you are interested in, such as pressure, strain, or any other parameter affecting the sensor response.

To calculate the sensitivity, we applied a perturbation to the parameter of interest and observe the resulting change in capacitance. This was done by varying the geometry, material properties, or boundary conditions associated with the parameter being investigated like- refractive index. We would then measure the resulting change in capacitance and calculate the sensitivity as the ratio of the change in capacitance to the change in the parameter.

COMSOL provides tools for parameter studies and post-processing that can assist in calculating sensitivities and visualizing the results. We plotted the capacitance as a function of the

parameter under investigation and analyzed the change in capacitance to determine the sensitivity.

It's important to note that the specific methodology for sensitivity calculation may vary depending on the exact configuration of the PCF sensor, the physical parameter being investigated, and the assumptions made in the simulation setup. Consulting the COMSOL documentation, tutorials, and examples related to electrostatics simulations and sensitivity analysis can provide further guidance on implementing these steps in COMSOL.

CHAPTER 3

DESIGN AND IMPLEMENTATION

3.1 STRUCTURAL DESIGN OF THE SENSOR

The proposed structure is presented in the paper and is shown in Figure 1. It was created using COMSOL Multiphysics 5.6. It is clear that there is an unidentified analyte layer positioned between the Perfectly Matched Layer (PML) and the exterior part of the cladding region for the purpose of external sensing. Both the outer part with the air holes and the PML, which serves as a material, both use silica.

Circular air holes, also known as air holes or air channels, are used in the design of optical fibers to create what is called a "holey" or "photonic crystal" fiber. This design offers several advantages over traditional solid-core fibers:

The circular air holes in photonic crystal fibers enable precise control over the modal properties of the guided light. By tailoring the size, shape, and arrangement of the air holes, it is possible to manipulate the propagation characteristics of light within the fiber. This control allows for the creation of specialty fibers with unique modal properties, such as single-mode fibers with large mode areas or fibers that support multiple modes simultaneously.

The arrangement of air holes in photonic crystal fibers can be designed to manipulate the dispersion properties of the guided light. By adjusting the size and spacing of the air holes, it is possible to achieve various types of dispersion, including normal dispersion, anomalous dispersion, or even zero dispersion at specific wavelengths. This control over dispersion is crucial in applications such as telecommunications, where it enables efficient transmission of information over long distances.

Photonic crystal fibers can exhibit enhanced nonlinear effects due to the confinement of light within the air-hole structure. The strong confinement of light in a small core area and the interaction of light with the high-index material surrounding the air holes can lead to increased nonlinear phenomena such as stimulated Raman scattering, four-wave mixing, and supercontinuum generation. These effects are exploited in applications such as nonlinear optics, optical frequency conversion, and broadband light sources.

By introducing specific asymmetries in the arrangement of air holes, photonic crystal fibers can be engineered to exhibit controllable birefringence. Birefringence refers to the property of having two different refractive indices for light polarized along different axes. Controllable birefringence is valuable in polarization-maintaining fibers used in applications like fiber optic sensing, interferometry, and telecommunications, where maintaining polarization state integrity is critical.

The use of circular air holes provides geometric flexibility in fiber design. The size, shape, and arrangement of the air holes can be varied to achieve specific performance characteristics. This versatility allows for the design of fibers optimized for various applications, including high-power laser delivery, high-resolution imaging, and specialty sensing applications.

Overall, the use of circular air holes in optical fiber design, as seen in photonic crystal fibers, enables precise control over modal properties, dispersion, nonlinear effects, birefringence, and geometric flexibility. These design capabilities make photonic crystal fibers suitable for a wide range of applications requiring advanced light-guiding functionalities.
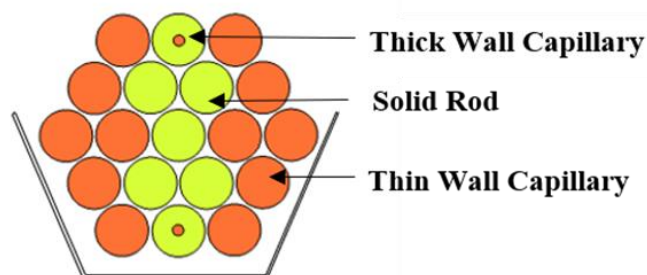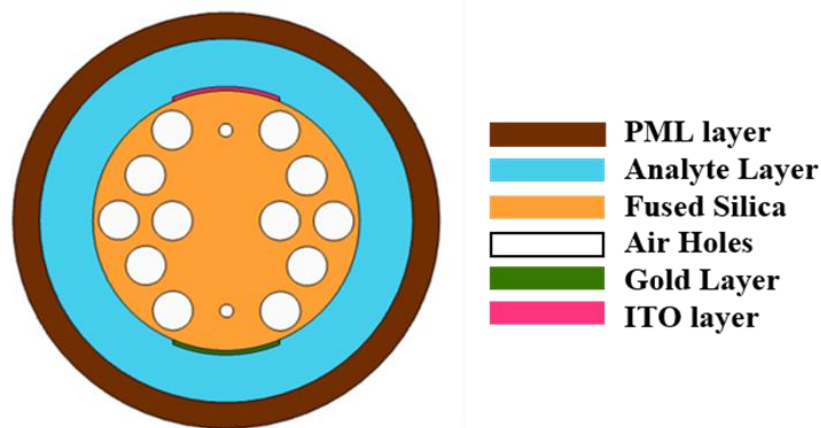
Fig 4: Illustration of the intended sensor's cross-sectional structure and the stacked preform used in the fabrication of the sensor.

3.1.1 Why Silica?

Silica has desirable properties that make it suitable for PML applications, such as its transparency to a wide range of wavelengths, low absorption, and low refractive index. These properties enable effective light transmission and minimize the loss of signal intensity. Additionally, silica is known for its stability and durability, making it a reliable material for long-term use in PML structures. It can withstand high temperatures, chemical resistance, and mechanical stress, ensuring the longevity and functionality of the PML. Furthermore, silica is readily available and cost-effective, making it a practical choice for implementing PML in various applications. Its widespread use and well-established manufacturing processes contribute to its popularity in the optical and photonics industries. Using the Sellmeier equation, the refractive index of Silica, $\eta(\lambda)$ has been determined [77] The equation is-

$$n^2(\lambda) = 1 + \frac{B_1\lambda^2}{\lambda^2 - C_1} + \frac{B_2\lambda^2}{\lambda^2 - C_2} + \frac{B_3\lambda^2}{\lambda^2 - C_3}$$

where RI of silica is n, the wavelength in μm is represented by λ . The Sellmeier coefficients were taken as B_1= 0.696163, B_2 = 0.408, B_3= 0.897479, C_1 = 0.0047μm², C_2 = 0.014μm², C_3=97.934μm² [78]

Two separate plasmonic layers with gold and ITO as the chosen plasmonic materials are positioned directly below the analyte layer and are set up in a certain configuration.

3.1.2 Why ITO?

ITO is preferred because of its high carrier density, which enables the realization of a tunable Localized Surface Plasmon Resonance (LSPR) wavelength in the near-infrared (NIR) range. ITO is chosen as a plasmonic material due to its unique properties, particularly its high carrier density and transparency in the visible to NIR range. Its high carrier density allows for efficient electron oscillations, contributing to strong plasmonic effects. The tunability of the LSPR wavelength is an essential consideration when selecting plasmonic materials. ITO offers the advantage of achieving a tunable LSPR wavelength in the NIR region. This tunability allows

for precise control over the interaction of light with the plasmonic structure, enabling applications such as biosensing, energy harvesting, and optoelectronic devices.

3.1.3 Why Gold?

Gold is chosen because of its outstanding chemical stability and non-reactivity. Gold is a popular choice for plasmonic materials due to its outstanding properties. One key advantage is its excellent chemical stability and inertness. Gold does not easily react with other substances, making it highly suitable for applications where stability and longevity are crucial. Another significant characteristic of gold is its ability to support localized surface plasmon resonance (LSPR), which refers to the collective oscillation of electrons on its surface when excited by incident light. Gold nanoparticles exhibit strong plasmonic effects in the visible to near-infrared (NIR) range, making them ideal for various sensing, imaging, and optical manipulation applications.

The ability of this suggested sensor to identify peaks in both x-polarization and y-polarization is its primary feature. In order to establish two phase matching requirements, the sensor model includes two materials that are geometrically positioned. The novelty of the sensor is demonstrated by the utilization of gold and ITO as plasmonic layers in this dual polarization study, especially when taking into account the refractive index (RI) range of 1.30 to 1.45.
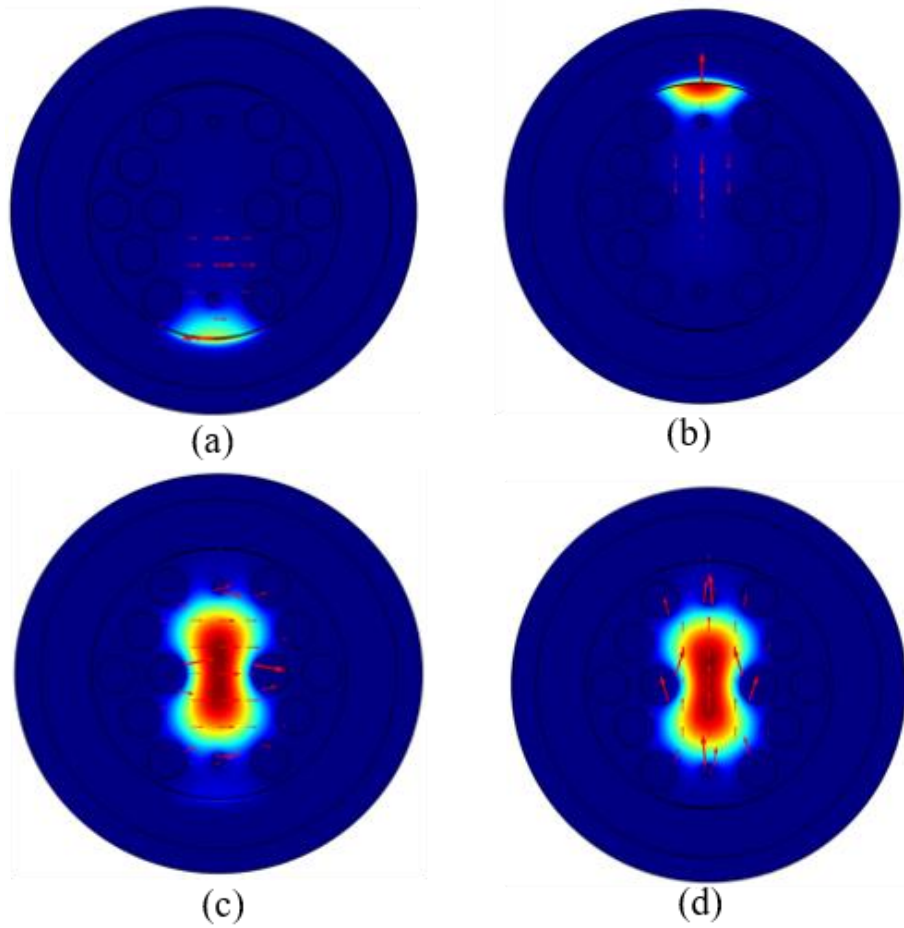
*Fig.5. **(a)** SPP-mode (Au), **(b)** SPP-mode (ITO), **(c)** x-polarized core-guided mode, **(d)** y-polarized core-guided mode*

In Fig. 5, the dark orange shaded region represents the area with the highest field intensity, while the dark blue region represents the area with the lowest field strength relative to the orange zone.

3.2 PERFORMANCE ANALYSIS:

In this section, the performance of the proposed sensor is discussed in terms of different sensing parameters and how minutely the sensor can detect an unknown analyte. Performance analysis of an optical sensor involves evaluating and quantifying its key characteristics and capabilities to determine how effectively it performs its intended function. The analysis aims to assess the sensor's performance in terms of accuracy, sensitivity, dynamic range, response time, reliability,

and other relevant parameters. Here are some aspects typically considered during the performance analysis of an optical sensor:

Sensitivity refers to the ability of the optical sensor to detect and measure the desired optical signal or parameter with precision. The sensor's sensitivity determines its ability to detect low-intensity signals or subtle changes in light levels accurately.

Accuracy relates to how closely the optical sensor's measurements correspond to the true values of the target parameter being sensed. It is essential to evaluate the accuracy of the sensor by comparing its measurements against known or calibrated reference values.

Linearity assesses how well the optical sensor's output responds in proportion to the input signal or parameter being measured. A linear response is desirable as it simplifies the interpretation and calibration of the sensor's measurements.

The dynamic range represents the range of optical power or signal levels over which the sensor can provide accurate measurements. A wide dynamic range allows the sensor to handle a broad range of input signals without saturation or loss of accuracy.

Resolution refers to the smallest change in the measured parameter that the optical sensor can detect and quantify. Higher resolution enables the sensor to detect small variations or changes with greater precision.

Response time indicates how quickly the optical sensor can react and provide a meaningful measurement in response to changes in the input signal or parameter. Fast response times are crucial for applications requiring real-time monitoring or rapid feedback.

Noise levels in the sensor's output can affect its accuracy and reliability. Performance analysis involves assessing the sensor's noise characteristics, including noise floor, signal-to-noise ratio, and stability over time. Lower noise levels and higher stability contribute to more reliable measurements.

Optical sensors may be subject to environmental factors such as temperature, humidity, vibration, and electromagnetic interference. Analyzing the sensor's performance under various environmental conditions helps evaluate its robustness and suitability for specific applications.

Optical sensors often require calibration to ensure accurate measurements. Performance analysis involves examining the calibration process, assessing the sensor's calibration stability over time, and determining the need for periodic recalibration.

The reliability and longevity of the optical sensor are crucial factors, especially in applications where the sensor is expected to operate continuously or in harsh conditions. Performance analysis may involve testing the sensor's durability, lifespan, and failure rates.

By conducting a thorough performance analysis, engineers and researchers can evaluate the strengths and limitations of an optical sensor, determine its fitness for specific applications, and make informed decisions regarding its deployment and optimization.

3.2.1 WS, DPPSS and AS

Wavelength sensitivity (WS), which refers to the change in resonance wavelength resulting from a variation or difference in the refractive index of the analyte, is a fundamental aspect of sensor performance [79]. Wavelength sensitivity (WS) is a measure of the change in resonance wavelength in response to variations or differences in the refractive index of the analyte. It quantifies the ability of a sensor to detect and respond to changes in the analyte's refractive index by measuring the shift in resonant wavelength. The wavelength sensitivity of an optical sensor refers to its ability to detect and respond to light at different wavelengths across the electromagnetic spectrum. It describes the sensor's sensitivity to different colors or wavelengths of light and indicates the range of wavelengths over which the sensor can effectively operate.

Optical sensors can be designed to be sensitive to specific wavelength ranges or operate across a broad spectrum. The sensitivity of a sensor is typically characterized by its spectral response curve, which shows the relationship between the sensor's sensitivity and the incident light's wavelength. Applications that require specific wavelength sensitivity include:

Spectroscopy: Optical sensors used in spectroscopic applications need to be sensitive to a wide range of wavelengths to analyze the composition, characteristics, and properties of substances. This includes applications such as chemical analysis, material identification, and environmental monitoring.

Telecommunications: Optical sensors used in fiber optic communication systems need to be sensitive to the specific wavelengths used for data transmission, typically in the near-infrared

range. These sensors enable the detection and conversion of optical signals in communication networks.

Biomedical and Life Sciences: Optical sensors used in biomedical and life sciences applications, such as fluorescence imaging, DNA sequencing, and flow cytometry, require sensitivity to specific wavelengths of light to detect and analyze biological samples and processes.

Environmental Monitoring: Optical sensors used in environmental monitoring applications, such as remote sensing and atmospheric research, need to be sensitive to specific wavelengths associated with the targeted environmental parameters, such as pollutant gases, aerosols, or vegetation health.

The sensitivity of any sensor can be quantified by measuring the maximum shift in resonant wavelength, as indicated by the following equation expressing WS.

$$S_w(\lambda) = \frac{\Delta \lambda_{Peak}}{\Delta n_a}$$

where, the difference between the resonant wavelengths is represented by $\Delta \lambda_{Peak}$ and the difference between analyte RI is represented by Δn_a.

The difference or variation in the resonance wavelength between two consecutive peaks in response to changes or differences in the refractive index of the analyte is referred to as the double polarization peak shift sensitivity (DPPSS). The DPPSS can be quantified using the following equation:

$$S_{DPPSS} = \frac{\left| \lambda_{x2} - \lambda_{y2} \right| - \left| \lambda_{x1} - \lambda_{y1} \right|}{n_2 - n_1}$$

where,

λ_{x2} = wavelength of peak of x polarization for greater RI

λ_{y2} = wavelength of peak of y polarization for greater RI

λ_{x1} = wavelength of peak of x polarization for lower RI

λ_{y1} = wavelength of peak of y polarization for lower RI

The variation in peaks due to confinement loss about variations in refractive index is referred to as amplitude sensitivity. It can be also explained as the sensitivity of the peaks to confinement loss resulting from variations in the refractive index is commonly referred to as amplitude sensitivity. The amplitude sensitivity of an optical sensor refers to its ability to detect and measure the amplitude or intensity of light. It represents the sensor's sensitivity to variations in the strength or power of the incident light signal.

Amplitude sensitivity is an essential characteristic of optical sensors as it determines the sensor's ability to accurately capture changes in light intensity. A high amplitude sensitivity means that the sensor can detect even small changes in light power, while a lower sensitivity may require stronger variations in light intensity to produce a measurable response. It captures the extent to which the amplitudes of the peaks change in response to fluctuations or differences in the refractive index and is stated in equation-

$$S(\lambda) = -\frac{1}{\alpha(\lambda, n_a)} \frac{\partial \alpha\ (\lambda, n_a)}{\alpha(\lambda, n_a)}$$

where, overall loss is indicated by $\alpha\ (\lambda,\ n_a)$, the two consecutive loss spectra's difference is indicated by $\partial \alpha(\lambda, n_a)$ and the required variation in analyte RI is ∂n_a.

The amplitude sensitivity of an optical sensor is crucial in various applications, including:

Photometry: Optical sensors used in photometric applications, such as light meters and photometers, need high amplitude sensitivity to accurately measure the intensity of light. This is important in fields like photography, film production, and light measurement for research or industrial purposes.

Sensing and Monitoring: Optical sensors utilized for sensing and monitoring applications, such as environmental monitoring, industrial process control, and biomedical sensing, require accurate detection of changes in light intensity. This includes monitoring variations in light levels, detecting changes in reflectivity or absorption, or sensing light-induced reactions.

Optical Communication: Optical sensors used in fiber optic communication systems need to accurately detect and measure the power of optical signals to ensure reliable data transmission.

This includes monitoring signal strength, detecting signal loss or attenuation, and optimizing signal levels in optical networks.

The amplitude sensitivity of an optical sensor determines its ability to detect and measure variations in light intensity accurately. It is an important characteristic to consider when selecting or designing sensors for applications that require sensitivity to changes in light power.

3.3 Optimization of geometrical parameters

The performance of the sensor is influenced by the geometrical parameters of the Photonic Crystal Fiber (PCF). These parameters play a significant role in determining the interaction between the evanescent field and the gold surface [77]. Therefore, it is crucial to carefully select these parameters, which include refractive index values, analyte layer thickness, PML layer thickness, larger and smaller air hole diameters, as well as the thickness of the gold and ITO layers.

To assess the sensor's performance, it is common practice to optimize various geometrical parameters and evaluate the sensor's behavior by altering the refractive index of the analyte. We can use optimization to find the geometrical parameter values that maximize the sensor's performance. We may optimize these settings to enhance the sensor's overall performance by boosting critical properties including sensitivity, resolution, and signal-to-noise ratio. Specific sensor properties may be needed for a variety of applications. We can modify the sensor's behavior to match the demands of a particular application or target analyte by adjusting the geometrical parameters. The sensor will function at its best within the required range of refractive index values thanks to this adjustment.

By changing the analyte's refractive index, we may assess how sensitive the sensor is to alterations in the environment. We can assess a sensor's capability to detect and measure fluctuations in analyte attributes, such as concentration or composition, by examining how it reacts to various refractive index values. By evaluating the sensor's behavior under different conditions, including varying refractive index values, we can assess its robustness, reliability, and accuracy. This evaluation provides insights into the sensor's overall performance characteristics and helps identify potential limitations or areas for improvement. Overall, by optimizing the analyte's refractive index and optimizing geometrical parameters, we can fine-

tune and examine the sensor's performance, personalize it for certain applications, test sensitivity, and evaluate its overall behavior and capabilities.

This optimization process involves keeping all parameters constant while varying one parameter at a time, a methodology employed by many studies in the field. Following this strategy, we conducted an investigation into the performance of our proposed sensor.

Initially, we set the gold film thickness and ITO layer thickness to 30 nm, the PML layer thickness to 1 µm, the larger hole radius to 0.75 µm, the smaller hole radius to 0.25 µm, and the refractive index to 1.37 before optimization. During the optimization process, we measured the confinement loss (CL) associated with these parameters and also quantified the Dual Polarization Peak Shift Sensitivity (DPPSS) at multiple lambda values for both x-polarization and y-polarization.

1) Optimization of ITO Layer

The ITO layer's thickness was tuned in the initial scenario shown in Fig 5. The ITO layer's thickness was adjusted in small stages from 30 nm to 1 nm while all other variables remained constant. The Double Polarization Peak Shift Sensitivity (DPPSS) was noted at each step. The analysis took into account wavelengths between 330 nm and 750 nm.
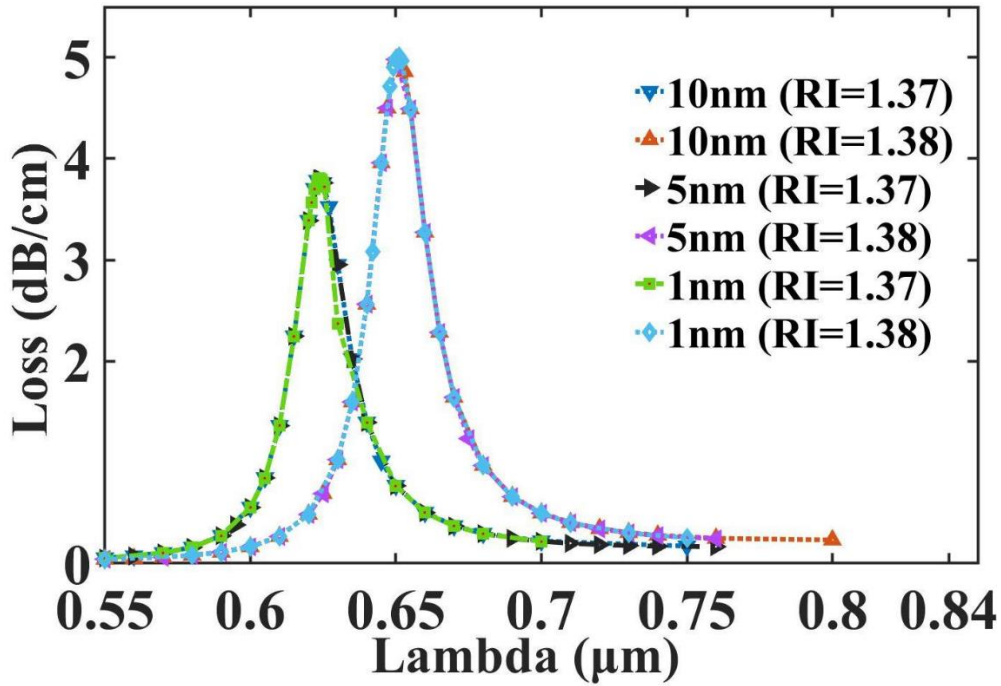
(a)
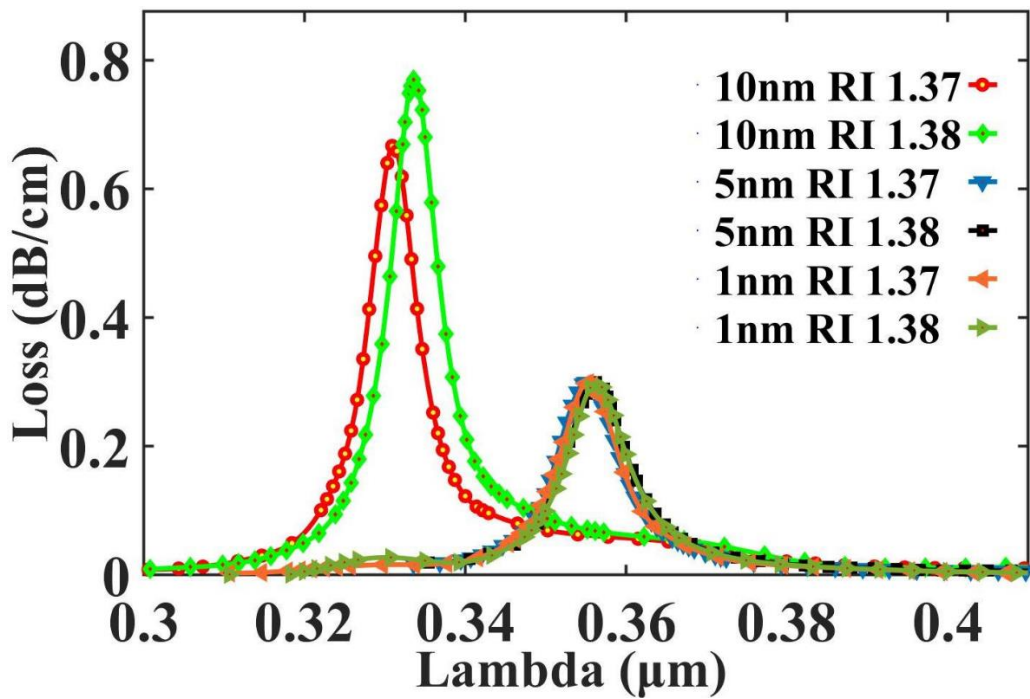
(b)

Fig 6: Effect of variation of ITO thickness (a) Loss due to Confinement in x-pol (b) Loss due to Confinement in y-pol for analyte with RI of 1.37 and 1.38

Upon comparing the results, we found that the maximum Double Polarization Peak Shift Sensitivity (DPPSS) achieved was 2630 nm/RIU (Table 1), and the maximum wavelength sensitivity reached 2720 nm/RIU at an ITO thickness of 1 nm. Based on these findings, we selected the optimized value of 1 nm for the thickness of the ITO layer in this design.

The expression given below was used to calculate confinement loss

$$\alpha_{loss} = 8.686 \times \frac{2\pi}{\lambda} \times I_m\left(\eta_{eff}\right) \times 10^4 \ dB/cm$$

where number of wave in the operating wavelength and in the free space is expressed by $2\pi/\lambda$ where λ is in μm range. We can extrapolate the value of $I_m\left(\eta_{eff}\right)$ which stands for the effective index's imaginary portion, from the simulation.

The optimization process involved considering both Double Polarization Peak Shift Sensitivity (DPPSS) and Wavelength Sensitivity (WS) for all the parameters. When the refractive index (RI) of the analyte increases, the WS also increases, resulting in a shift towards higher wavelengths, indicating a peak point shift. However, it was observed that the optimization of the ITO layer did not significantly impact the x-polarization (x-pol) response.

2) Optimization of the Au Layer

The thickness of the Au layer significantly influences the confinement loss, peak shifting at the resonant wavelength, and the sensing capability of SPR (Surface Plasmon Resonance) sensors, which is widely acknowledged [80]. To explore the dominance of Au on the sensing performance while maintaining the optimal ITO value, the thickness of the gold layer was varied from the initial value of 30 nm to 60 nm.

Observations revealed that increasing the thickness of the gold layer led to a reduction in confinement loss and a shift of the resonance peak towards longer wavelengths. This relationship is depicted in Fig 6. Notably, the Double Polarization Peak Shift Sensitivity (DPPSS) decreased as the Au thickness increased from 55 nm to 60 nm. At 55 nm, Au (x-pol) exhibited a low loss of 0.85 dB/cm for RI=1.37 and 1.11 dB/cm for RI=1.38, with the maximum DPPSS at RI=1.37 measuring 3725 nm/RIU (Table 1). Thus, the Au thickness of 55 nm was considered the most favorable among all the thicknesses examined.

Moreover, it is important to note that higher thicknesses of Au pose challenges for light penetration through the plasmonic layers, resulting in reduced confinement loss and sensitivity.
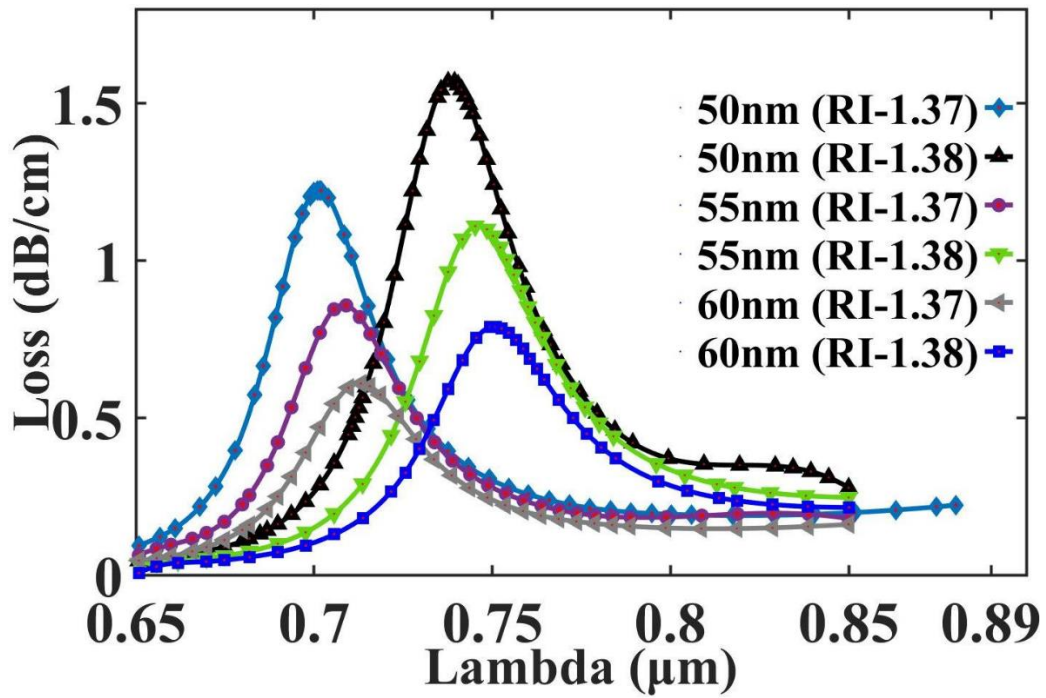
(a)
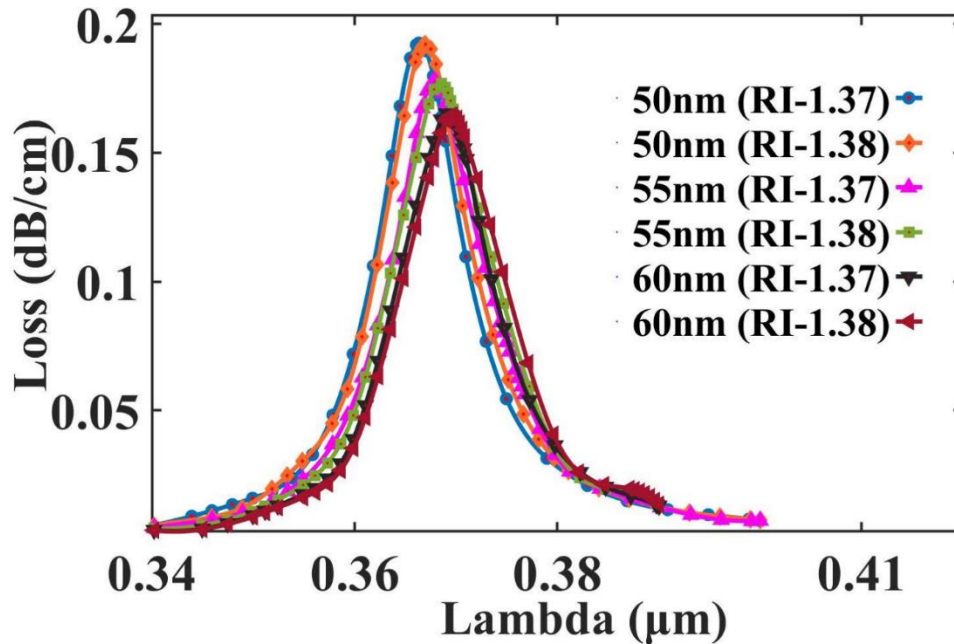
(b)

Fig 7: Impact of variation of Au thickness (a) Loss due to confinement in x-pol (b) Loss due to confinement in y-pol for analyte with RI of 1.37 and 1.38

3) Optimization of Bigger Air Hole Radius

In this design, the first inner circle of the structure (Fig. 7) contains air holes of two different sizes. These air holes play a crucial role in modifying the refractive index of the core-guided mode, thereby influencing the phase matching between the Surface Plasmon Polariton (SPP) mode and the Core-guided mode.
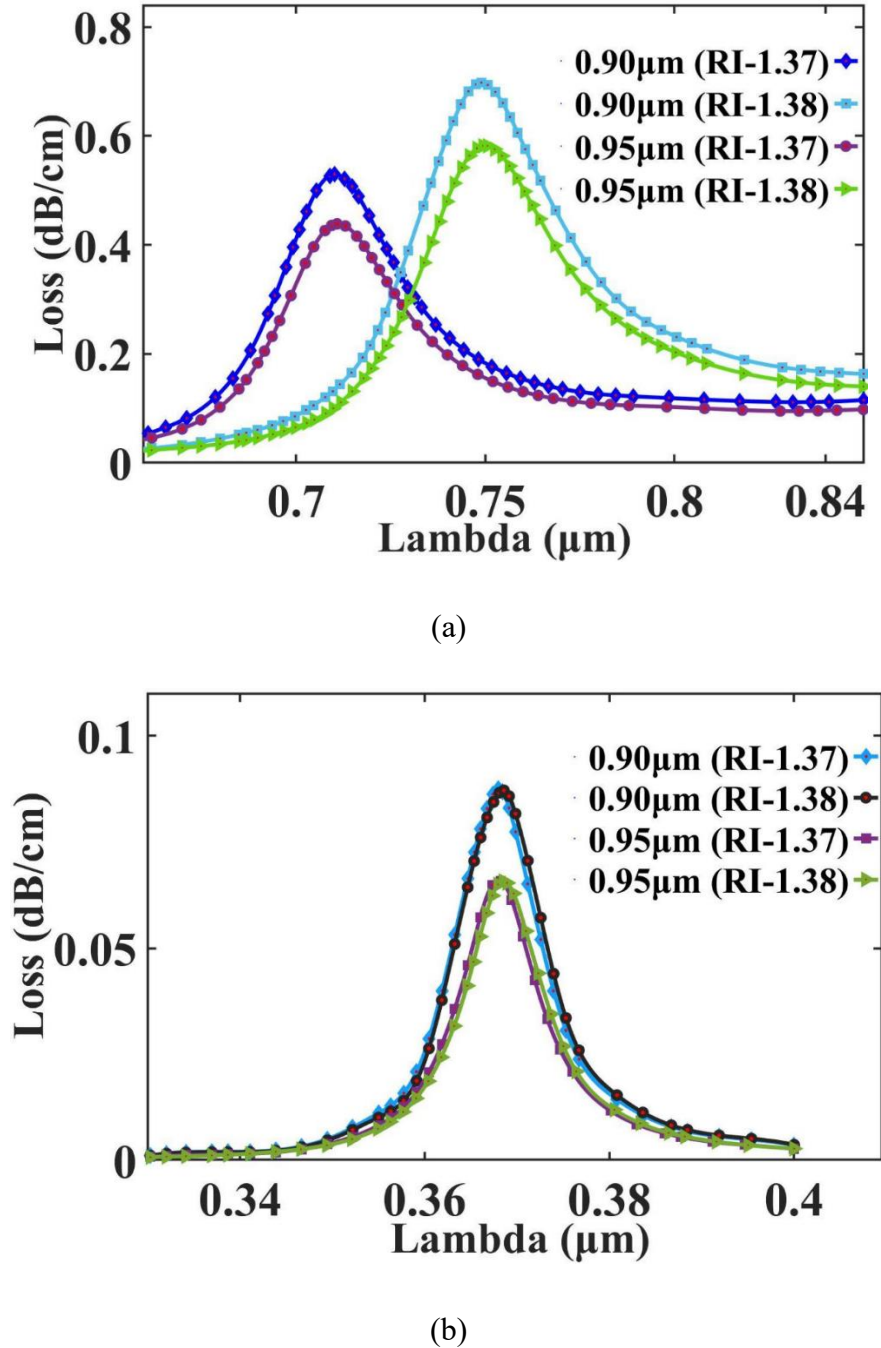

(a)

(b)

Fig 8: Impact of variation in bigger air hole radius(a) Loss due to confinement in x-pol (b) Loss due to confinement in y-pol for analyte with RI of 1.37 and 1.38

Examining Fig 8, it can be observed that changes in the radius of the larger air hole do not significantly impact the sensitivity and confinement loss. This can be attributed to the specific placement of these air holes within that radius and their role in generating the surface plasmon waves (SPW) [17].

To explore the effect of the radius, it was adjusted between 0.75 µm and 1 µm within the wavelength range of 330 nm to 800 nm. The maximum Double Polarization Peak Shift Sensitivity (DPPSS) obtained was 3840 nm/RIU at a radius of 0.95 µm (Table 1).

4) Optimization of the Smaller Air Hole Radius

The radius of the smaller air holes was adjusted within the range of 0.25 µm to 0.15 µm. Upon analysis, it was found that the maximum Double Polarization Peak Shift Sensitivity (DPPSS) was achieved at a radius of 0.2 µm, measuring 3845 nm/RIU (Table 1).

It was observed that increasing the radius of the smaller air holes resulted in a significant reduction in confinement loss, primarily due to the damping effect (Fig 9). As the radius increases, the distance between the air holes decreases, leading to decreased light penetration in the core mode. Consequently, the confinement loss experiences a notable decrease.

Furthermore, it can be observed from Figure 9 (b) that the variation in the radius of the smaller air holes does not contribute significantly to the y-polarization modes.
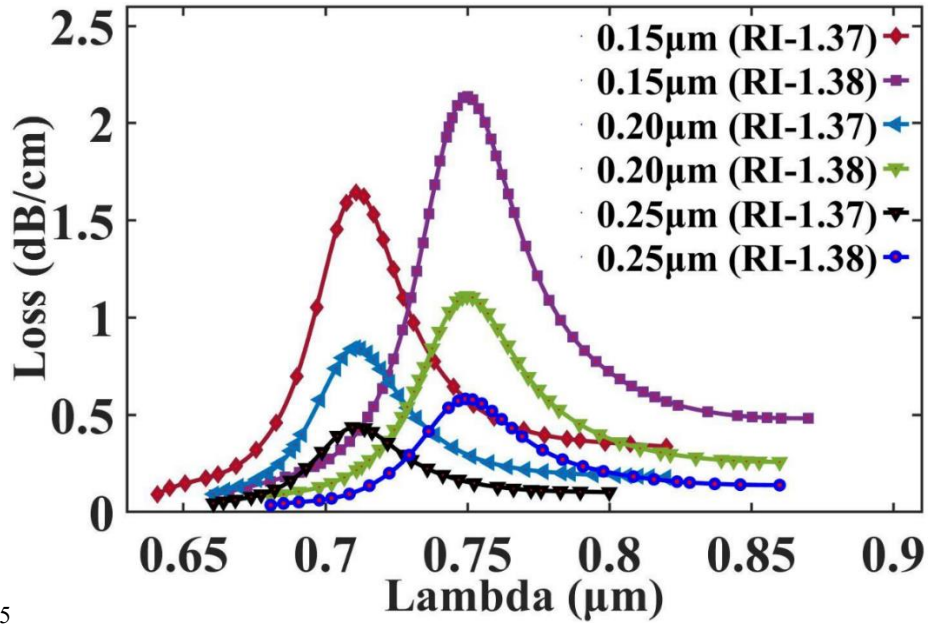
(a)
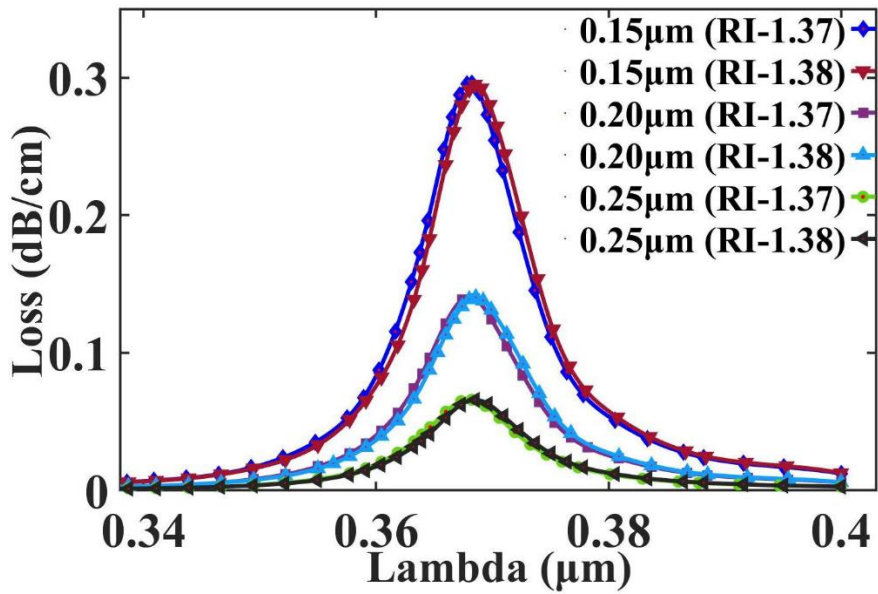
(b)

Fig 9: Impact of variation of smaller air hole radius (a) Loss due to confinement in x-pol (b) Loss due to confinement in y-pol for analyte with RI of 1.37 and 1.38

Table.1. Optimization of different parameters with respect to DPPSS at analyte RI 1.37.

| Parameter	Dimension	Peak CL (dB/cm)		DPPSS (nm/RIU)
		x-pol	y-pol	
ITO thickness (Fig.3)	10 nm, 5 nm, 1 nm	3.785, 3.803, 3.803	0.667, 0.299, 0.298	2430, 2450, 2630
Au thickness (Fig.4)	50 nm, 55 nm, 60 nm	1.223, 0.859, 0.610	0.192, 0.177, 0.165	3640, 3725, 3710
Bigger Air Hole Radius (Fig.5)	0.85 μm 0.90 μm, 0.95 μm	0.629 0.529, 0.438	0.113 0.087, 0.066	3800, 3835, 3840
Smaller Air Hole Radius (Fig.6)	0.15 μm, 0.20 μm, 0.25 μm	1.644, 0.845, 0.438	0.296, 0.140, 0.066	3830, 3845, 3840

CHAPTER 4

RESULT ANALYSIS

4.1 Sensing Performance for Different RI:

The performance evaluation of the sensor involves studying the confinement loss of different analytes with varying refractive indices. By analyzing the shift in the resonance peak, it becomes possible to discern the identity of unknown dielectric materials based on the subtle changes observed in the surface plasmon polariton (SPP) mode within the effective refractive index (RI) range. [77]. In this study, confinement loss was measured for analytes exhibiting refractive indices ranging from 1.30 to 1.41.

The refractive index (RI) range of 1.30 to 1.41 is important in the context of the study or sensor design because it covers a range of common materials and analytes encountered in various applications. In many biological and chemical systems, the refractive index of the surrounding medium or the analyte of interest falls within this range. For example, the refractive index of biological fluids like white blood cells (1.36), human liver (1.369), blood plasma (1.35), human urine concentration (1.3415–1.3464), human intestinal mucosa (1.329–1.338), red blood cells (1.40), hemoglobin (1.38), or cell culture media typically lie within this range. Similarly, many common chemicals, biomolecules, and analytes exhibit refractive indices within this range [29]

Analyte identification with precise refractive index (RI) values is critical for fields such as organic chemistry analysis, food quality assessment, and disease diagnostics. A higher level of RI detection precision offers increased sensitivity, enabling the identification of certain substances, the assessment of food quality, and the early detection of diseases. Developing precise RI measuring techniques is critical for progress in these sectors [25]

Examining Figure 9 reveals a fascinating characteristic: the x-polarization exhibits a deeper penetration depth of the electric field from the center than the y-polarization. As a result, the confinement loss reported during x-polarization is greater than that reported during y-polarization. The difference between the two polarizations in field penetration and confinement loss emphasizes the complex interplay between the polarization direction of the incident light and its interaction with the dielectric medium.

Additionally, a noteworthy and important result is the substantial improvement seen in the Double Polarization Parameter for Sensitivity (DPPSS) as the refractive index rises. This is demonstrated by the resonant peak shifting towards longer wavelengths, which shows a unique red shift phenomenon accompanying the increase in RI.
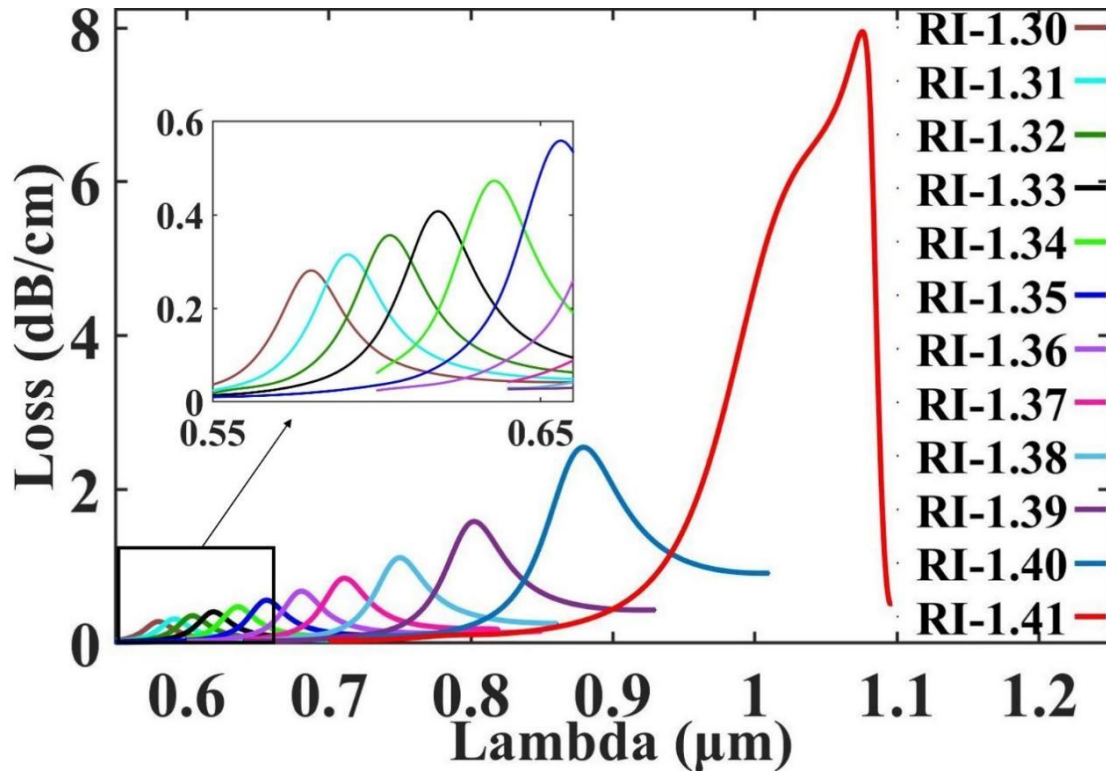
(a)
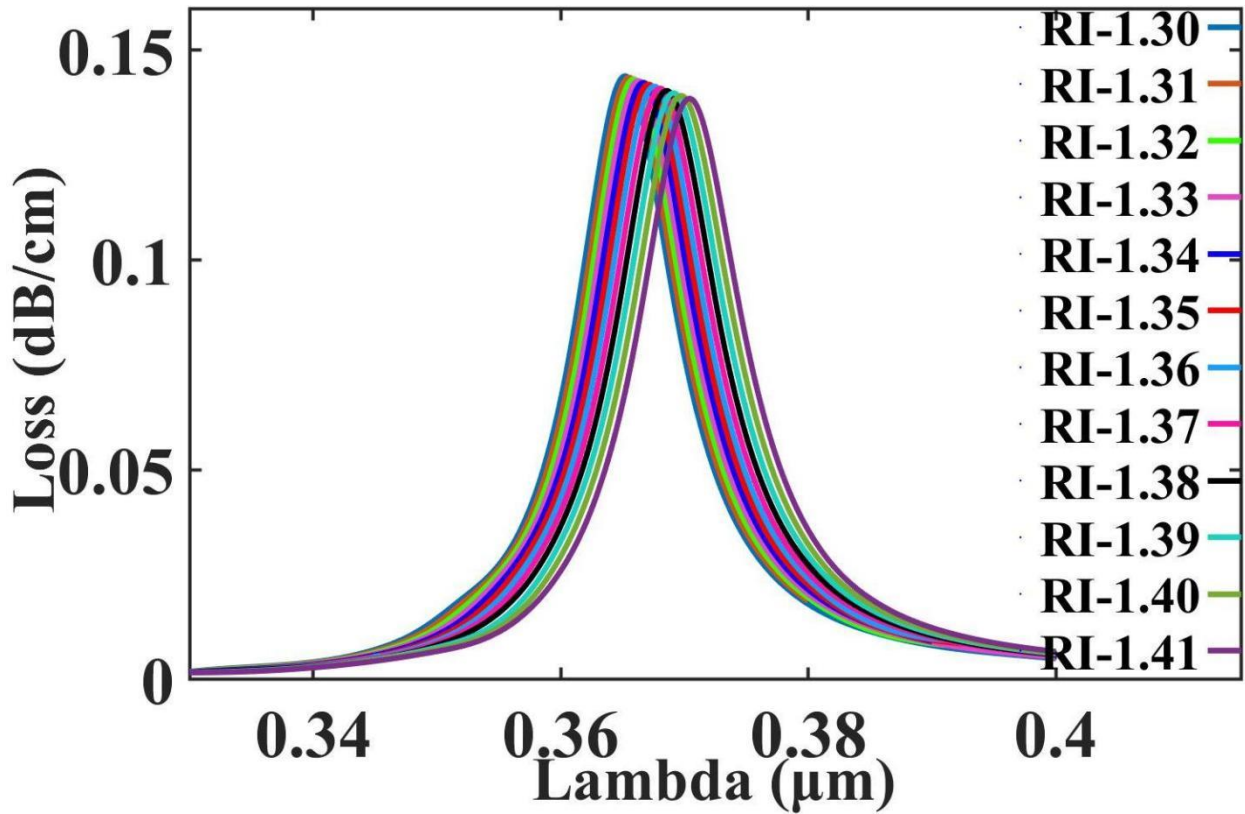
(b)

Fig 10: Loss due to Confinement (a) for x-pol within RI span 1.30-1.41 and (b) for y-pol within RI span 1.30-1.411

The red shift property can provide important details about a system's structural, chemical, and physical properties. It functions as a diagnostic tool for studying fundamental phenomena, characterizing materials, and designing sensitive sensing systems. At the extremities of the refractive index (RI) range (RI 1.40), the DPPSS value exhibits a significant increase, reaching 19560 nm/RIU. These results show a significant improvement in the sensor's performance and sensitivity, offering important information on how the system reacts to RI variations throughout the whole range.

Different performance parameters of this sensor, especially confinement loss, wavelength sensitivity and DPPSS for different analyte refractive indices are analyzed and mentioned in tabular form in Table.2.

50

Table.2. Analysis of the Performance of Sensing with respect to Wavelength Sensitivity and DPPSS by varying analyte RI

Analyte RI	Confinement Loss(dB/cm)		Wavelength Sensitivity nm/RIU	DPPSS nm/RIU
	x-pol	y-pol	x-pol	
1.3	0.281	0.143	1130	1100
1.31	0.315	0.143	1270	1230
1.32	0.356	0.143	1480	1440
1.33	0.407	0.142	1720	1720
1.34	0.472	0.141	2000	1920
1.35	0.558	0.141	2470	2430
1.36	0.676	0.141	3030	2975
1.37	0.845	0.140	3890	3845
1.38	1.110	0.140	5250	5190
1.39	1.581	0.139	7680	7620
1.4	2.547	0.139	19630	19560
1.41	7.952	0.138	-	-

4.2 DPPSS and AS Trade Offs:

Because the optimization procedure concentrates on maximizing the Double Polarization Parameter for Sensitivity (DPPSS) rather than AS, the sensor's amplitude sensitivity (AS) is purposefully maintained low in this design. Prioritizing DPPSS reduces the wavelength shift in the loss curve, which lowers the AS value.

(a)
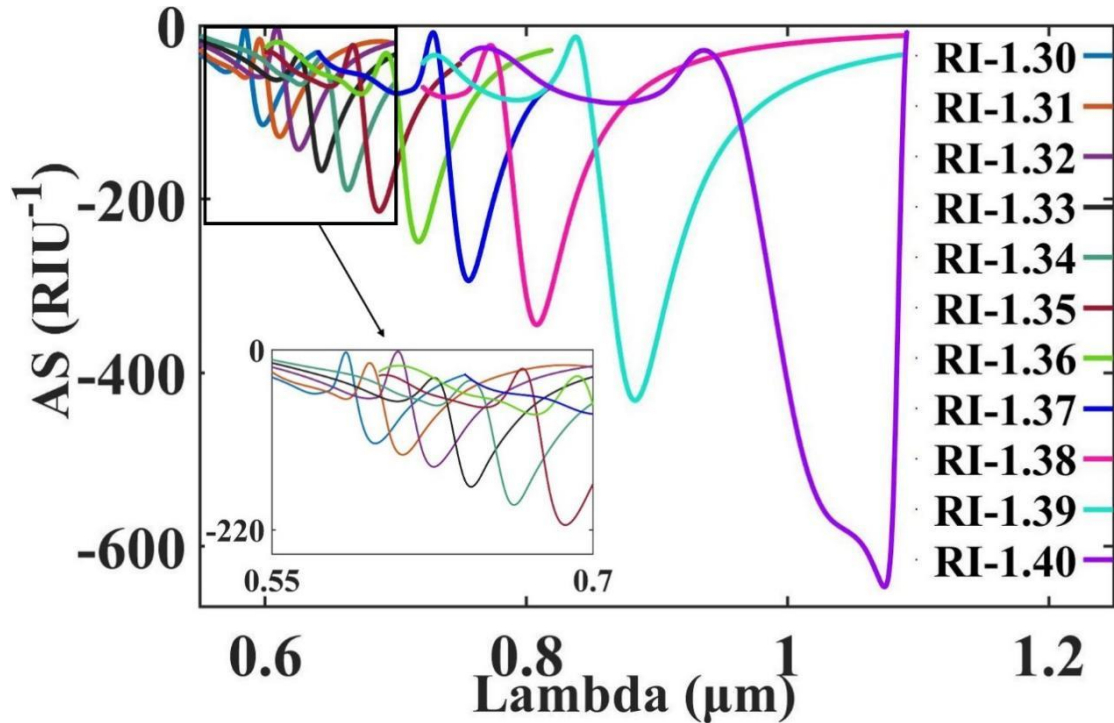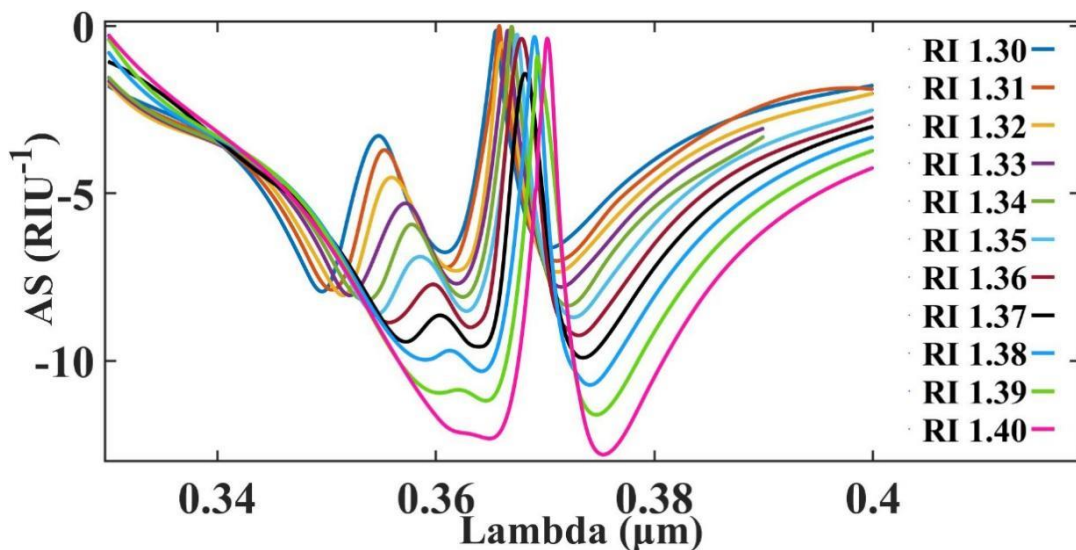
Fig 11: Amplitude sensitivity (a) for x-pol amidst RI band of 1.30-1.40 and (b) for y-pol for the refractive index range between 1.30-1.40

(b)

Fig 11 shows the AS for two distinct polarizations. The design achieves a maximum AS of 646.18 RIU-1. This deliberate choice allows for a trade-off between amplitude sensitivity and the overall performance of the sensor in terms of its sensitivity to refractive index variations.

4.3 Some Features of the Sensor

The proposed sensor has some properties that make it unique. DPPSS is one of them. It is a completely new concept that has been discussed in this work where both the polarizations has been taken into account.

4.3.1 Novel DPPSS Technique and its Significance:

The Double Polarization Peak Shift Sensitivity (DPPSS) is a unique metric that incorporates the resonant wavelength values of both the x and y polarizations for successive refractive index (RI) values, giving a thorough assessment of the sensor's sensitivity. The significance of such sensor is given below:

1. When calculating the sensitivity of the SPR sensor, the DPPSS can be determined by considering changes in both x and y polarization. This unique feature sets DPPSS apart from conventional parameters by encompassing the full extent of polarization effects in SPR sensor measurements. By incorporating both x and y polarizations, DPPSS offers a comprehensive and holistic approach to quantifying the sensitivity of the sensor, paving the way for enhanced precision and accuracy in SPR sensing applications.

2. The proposed design showcases intriguing characteristics of the materials employed, namely Indium Tin Oxide (ITO) and Gold (Au). During the optimization process, the resonance peak shift exhibited an intriguing behavior in response to different polarizations. Specifically, in Figure 5 (a), it was observed that the resonance peak shift in ITO did not respond to x-polarized light, while in Figure 4a, with the change of Au layer, we observe a major shift of resonance peak of x polarization and no shift in the resonance peak was observed for y-polarized light [Fig 4 (b)].

3. This finding eliminates the need to rely entirely on a single polarization for reliable measurements. The ability to leverage the distinct behaviors of the materials with respect to different polarizations not only enhances the sensitivity but also offers a novel

method for obtaining valuable information about analytes and their molecular interaction.

4.3.2 Increased Wavelength:

In the optimization process, the wavelength range of 0.3 µm to 0.85 µm was considered for the sensor design. During the optimization, it was observed that the resonant peak for y-polarization remained within the range of 0.3 µm to 0.4 µm, while for x-polarization, it shifted within the range of 0.6 µm to 0.8 µm.

This finding has significant implications because it shows that the same sensor design may successfully employ both polarizations. The overall wavelength range of the sensor is increased by taking use of the different wavelength ranges for each polarization. This improved flexibility and variety in sensing applications enables for the identification of analytes from the infrared to visible spectrum. Increasing the wavelength range of an optical sensor can benefit its performance and expand its capabilities in several ways:

By extending the wavelength range, the optical sensor can capture and detect a wider range of wavelengths, enabling it to work across a broader portion of the electromagnetic spectrum. This is particularly advantageous in applications that involve the detection and analysis of light across various wavelengths, such as spectroscopy, remote sensing, and hyperspectral imaging.

A sensor with an increased wavelength range can be utilized in a broader range of applications and environments. It can accommodate different light sources and target materials that emit, absorb, or scatter light at different wavelengths. This versatility allows the sensor to be used in diverse fields, including telecommunications, environmental monitoring, biomedical sensing, and industrial process control.

Certain applications require simultaneous or sequential sensing at multiple wavelengths. For example, in biomedical sensing or fluorescence imaging, detecting and analyzing specific fluorescence signals emitted at different wavelengths can provide valuable information about

cellular activity or molecular interactions. A wide wavelength range allows the sensor to cover multiple fluorescence channels or other spectrally distinct signals simultaneously.

Different phenomena and substances exhibit unique spectral characteristics and features at specific wavelengths. By extending the wavelength range, the sensor can detect and differentiate these characteristics with higher sensitivity and resolution. This is beneficial in applications like gas sensing, where different gases exhibit distinct absorption or emission lines at specific wavelengths, allowing for precise identification and quantification.

Increasing the wavelength range can open up possibilities for new applications and research areas. It enables exploration of novel sensing techniques, emerging optical phenomena, and new materials that interact with light in previously unexplored wavelength regions. This promotes innovation and encourages advancements in various scientific and technological fields.

In many cases, optical systems, devices, or light sources operate at specific or standardized wavelength ranges. By increasing the wavelength range of the sensor, it can be better integrated into existing systems without the need for extensive modifications or adaptations. This compatibility facilitates seamless integration and enhances the sensor's applicability and adoption in real-world scenarios.

It's important to note that increasing the wavelength range of an optical sensor may also present challenges, such as the need for broader spectral calibration, potential noise sources, and the design and selection of appropriate photodetection materials. However, the overall benefits of an increased wavelength range often outweigh these considerations, making it a valuable characteristic for optical sensors in various applications.

4.3.3 Potential Application of the Sensor:

The DPPSS parameter of a SPR sensor can give complementary information about molecular interactions occurring at sensor interface. It is possible to examine the variations in refractive index and the degree of molecule binding for each polarization separately by monitoring the two polarizations simultaneously. Therefore, our proposed sensor can be used in analyzing biological samples containing multiple interacting components such as serum, whole blood cell

etc. It also has the potential in material science exploring interactions of different materials in different polarizations, thus, enhancing the reliability of the sensor.

With the increase in the range of wavelength, the sensor can be used for multiple applications. Modulators and waveguides in integrated optics, subwavelength waveguiding, nearfield optical microscopy, SPR analysis and surface-enhanced Raman scattering for the label-free detection of biological molecules are some of the current applications of plasmonic.[81]Use of plasmonic in the mid wavelength-infrared region has a great role in emitters, chemical sensing surfaces and improved IR detectors [82]

Because of their resonance frequency in the regions like - visible and near-infrared, noble metal nanoparticles (NPs) have a well-known LSPR phenomenon that is being researched to develop different sectors like biomedical, energy, and information technology areas. This includes fields of bioimaging, and analysis of micro-organisms like in biosensing. The application area is widespread into data storage, nano surgery and photocatalysis too [83]

ITO has been advantageous for the wavelength range of the near-infrared region to the visible region for its broader NIR absorbance and smaller size [30]. Therefore, a huge area of applications is made possible due to the combination of gold and ITO in SPR sensors.

Optical sensors find numerous applications across various industries due to their ability to detect and measure light or electromagnetic radiation. Here are some common applications of optical sensors:

Proximity and Motion Detection: Optical sensors can be used to detect the presence or absence of an object or to determine its motion. They are often employed in automatic doors, security systems, robotics, and motion-activated lighting systems.

Ambient Light Sensing: Optical sensors can measure the intensity of ambient light in the surrounding environment. This feature is frequently used in smartphones and tablets to adjust the brightness of the display according to the lighting conditions, enhancing user experience and conserving battery life.

Optical Fiber Communication: Optical sensors play a vital role in optical fiber communication systems, enabling the transmission of large amounts of data over long distances. They are used to convert light signals into electrical signals and vice versa, facilitating high-speed and reliable communication.

Spectroscopy: Optical sensors are extensively utilized in spectroscopic applications to analyze the composition and characteristics of substances. Spectrometers equipped with optical sensors are employed in fields such as chemistry, biology, environmental monitoring, and pharmaceuticals.

Biomedical Sensing: Optical sensors find applications in the medical and healthcare sectors for various purposes. They can be used for non-invasive blood oxygen level monitoring (pulse oximetry), glucose sensing, flow cytometry, DNA sequencing, and imaging techniques like optical coherence tomography (OCT) or fluorescence microscopy.

Imaging and Photography: Optical sensors are used in digital cameras, smartphones, and imaging devices to capture light and convert it into digital signals. They enable the detection of colors, patterns, and details, forming the foundation of modern photography and imaging technology.

Industrial Automation: Optical sensors are employed in industrial automation systems for tasks such as product inspection, object counting, and quality control. They can detect defects, measure dimensions, and ensure proper alignment of components.

Environmental Monitoring: Optical sensors are utilized for monitoring and measuring various environmental parameters. They can assess air quality, detect pollutants, measure water turbidity, and monitor weather conditions by detecting light intensity, wavelength, or scattering properties.

Automotive Applications: Optical sensors are used in automotive systems for tasks such as ambient light sensing, rain detection, obstacle detection, and adaptive headlights. They enhance safety, improve driving experience, and assist in autonomous driving technologies.

Aerospace and Defense: Optical sensors are employed in aerospace and defense applications for tasks like missile guidance, target tracking, remote sensing, and surveillance. They can detect and analyze light emitted or reflected from objects of interest, enabling advanced reconnaissance and navigation capabilities.

These are just a few examples of the many applications of optical sensors across various industries. The versatility and precision of optical sensing technology make it an essential component in numerous fields.

4.4 Fabrication

There is an emphasis on designing sensors with increased sensing capabilities and easier manufacturing techniques in the case of optical fiber designs, notably for PCF SPR sensors. One technique is to carefully plan the configuration of air chambers within the PCF. The suggested sensor architecture has a hexagonal array of circular air chambers. The design of these air holes is carefully selected to maximize sensor functionality while maintaining feasible fabrication steps. Here are some details that highlight the significance of this design:

Enhanced Sensing Capabilities:
The hexagonal layout of air chambers gives various advantages for sensing applications. For starters, it has a high surface-to-volume ratio, which enhances interaction between the sensing medium and the guided light within the fiber. This enhances the sensitivity of the sensor, allowing for more precise detection of analytes or biomolecular interactions.

Improved Light Confinement:
The strategic arrangement of the air cavities aids in confining light within the fiber core, boosting contact with the sensing region. This confinement may be modified to increase the sensor's resolution and accuracy.

Fabrication Ease:
The suggested sensor design takes fabrication ease into account. When compared to more complicated arrangements, employing a hexagonal structure simplifies the construction process. The pattern's regularity allows for more control over the placement of the air cavities during the fabrication process, limiting the possibility of faults or inconsistencies.
The flowchart outlined in Fig.11 are the steps for creating the preforms and drawing the PCFs.

Capillary Tube Stacking: Capillary tube stacking is an important stage in the creation of the PCF preform. In order to create the PCF preform, several capillary tubes (thick walled and thin-walled capillary) were stacked. All these capillaries of the sensor that is proposed, together with solid rods, will be positioned in accordance with the air hole layout which is shown in Fig.10.

Jacketing and collapsing: Jacketing with big tubes is used to protect the capillary tubes and retain their structure throughout following processing processes. This aids in the prevention of capillary distortion or injury. Additionally collapsing process maybe applied to fuse the capillaries together and create a consolidated preform [84].
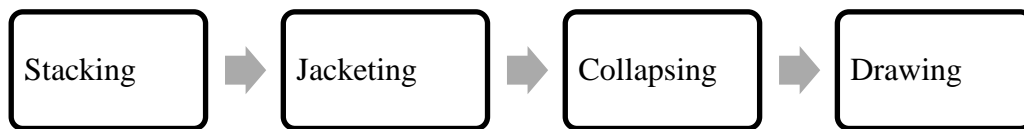
| Stacking | → | Jacketing | → | Collapsing | → | Drawing |

Fig 12: Fabrication flowchart of PCF using stacking and drawing method

Drawing Preform: The cane, or intermediate preform, created from the capillary stacking and jacketing process is subsequently drawn down to the necessary PCF dimensions. This involves pulling the preform through a heated furnace, which reduces its diameter and elongates it to the desired length.

1. **Photolithography for ITO and Gold Layers:** A two-step photolithography method is used to build the conductive layers required for the sensor. Photolithography is a process that defines precise patterns on a substrate by using light-sensitive materials (photoresists) and masks. It is employed to build the Indium Tin Oxide (ITO) and gold layers on the fiber surface. By employing the chemical vapor deposition (CVD) method, one plasmonic coating will initially be placed on to the fiber surface. Following that, plasmonic layer 1 will be achieved by applying a mask to the desired region. The construction of plasmonic layer 2 will follow a similar approach.
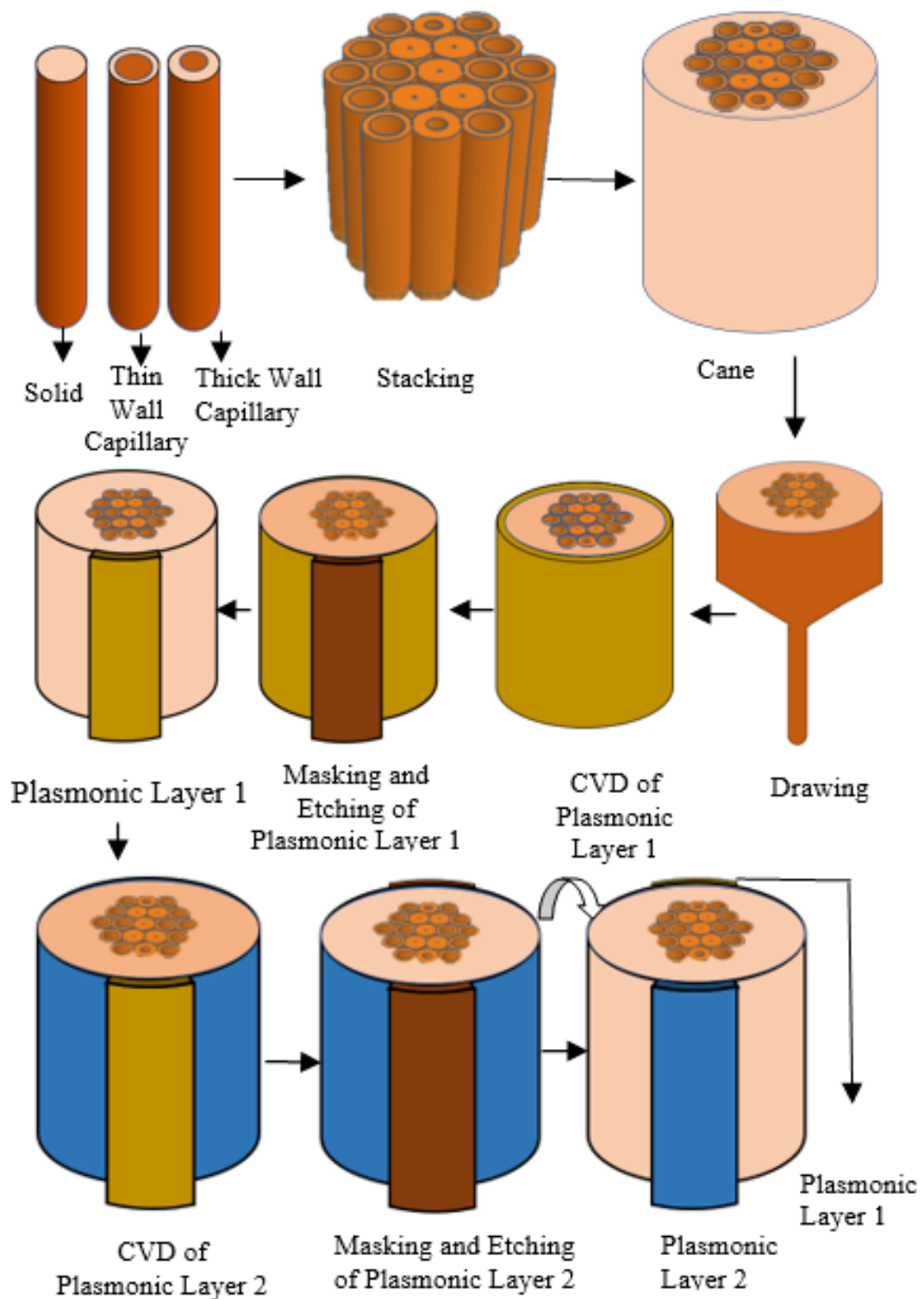
Fig 13: Prospective fabrication order of the Sensor

Two pumps will be utilized to implement the sensing layer, one for introducing analytes into the layer, another for extracting analytes out of the layer.

4.5 Analysis of Fabrication Tolerance

Obtaining accurate dimensions for the PCF SPR sensor during the fabrication process can be difficult, and variations from the ideal structure are common. To account for these variances, a fabrication tolerance (FT) analysis is required to quantify the impact of these discrepancies on sensor performance.

The FT analysis focuses on two elements in the specific design mentioned: the ITO film thickness and the air hole radius. A variety of fabrication-related flaws are taken into consideration by allowing for deviations of between 5% and 10% from these parameters' ideal values.

While making the sensor, these fabrication approaches cannot reach an accurate dimension all the time. There are always 1% or 2% deviations from the target structure dimensions, necessitating fabrication tolerance (FT) study. In this design, we have chosen to modify ITO film thickness and smaller air hole radius by ±5% and ±10% from their optimum value, thus we will be able to account for a wide range of fabrication-related defects.

Figure 11 shows the influence of these adjustments on the sensor's resonant wavelength (RW), Wavelength Sensitivity (WS), and Double Polarization Peak Shift Sensitivity (DPPSS). The results show that parameter changes of 5% to 10% have no effect on the resonant wavelength, thus making no alterations in WS and DPPSS. This implies that the sensor's resonant properties and detection capabilities can be maintained even if the ITO film thickness deviates within the prescribed tolerance range. Again, for smaller air hole radius, we see slight difference in CL which is observed in all RIs, thus it can be neglected.

Based on these findings, it can be concluded that manufacturing defects have no major impact on sensor performance. Deviations from the target structural dimensions within the given tolerance range (5% and 10%) have no discernible effect on resonant wavelength, sensitivity or DPPSS. Therefore, we may infer that our sensor performance won't have any significant deviations than the reported values due to fabrication error.
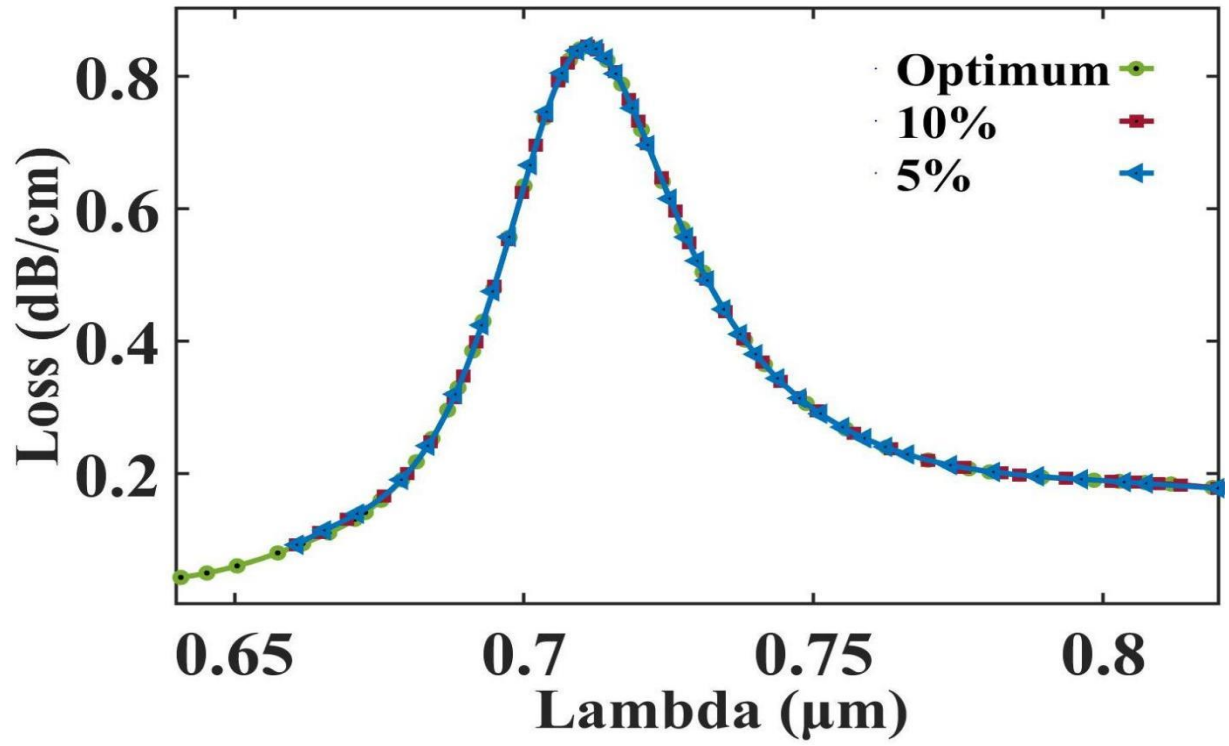
(a)
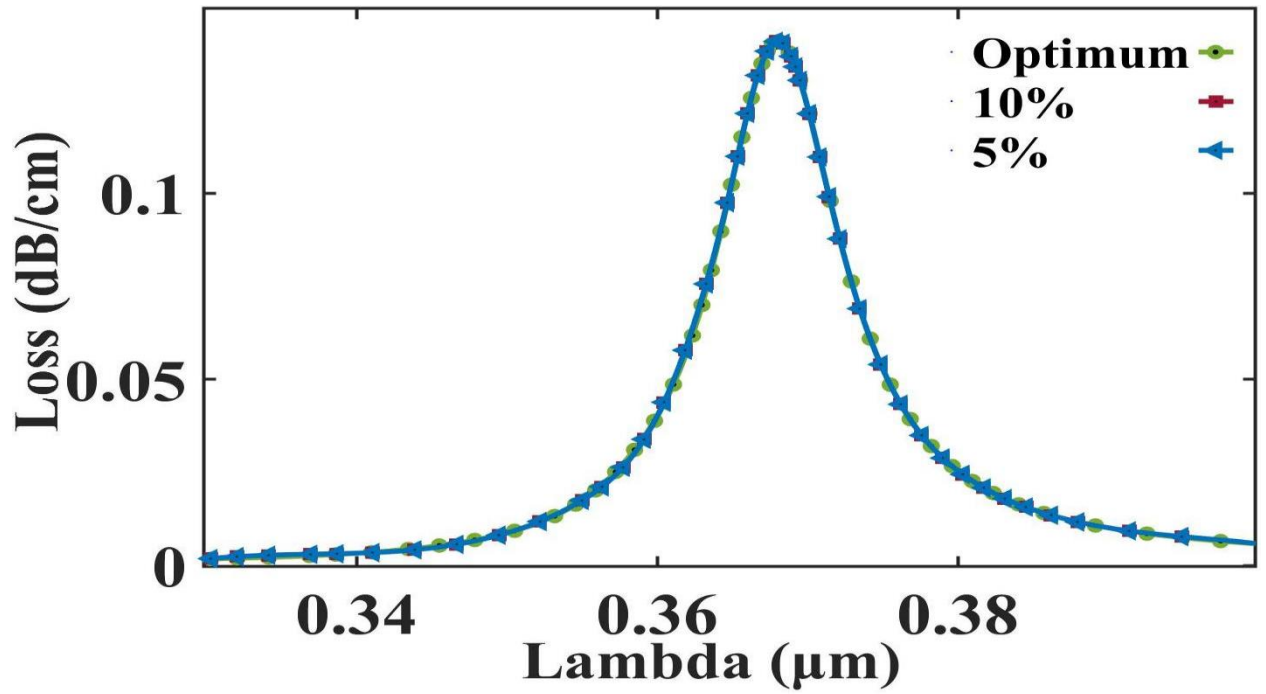
(b)
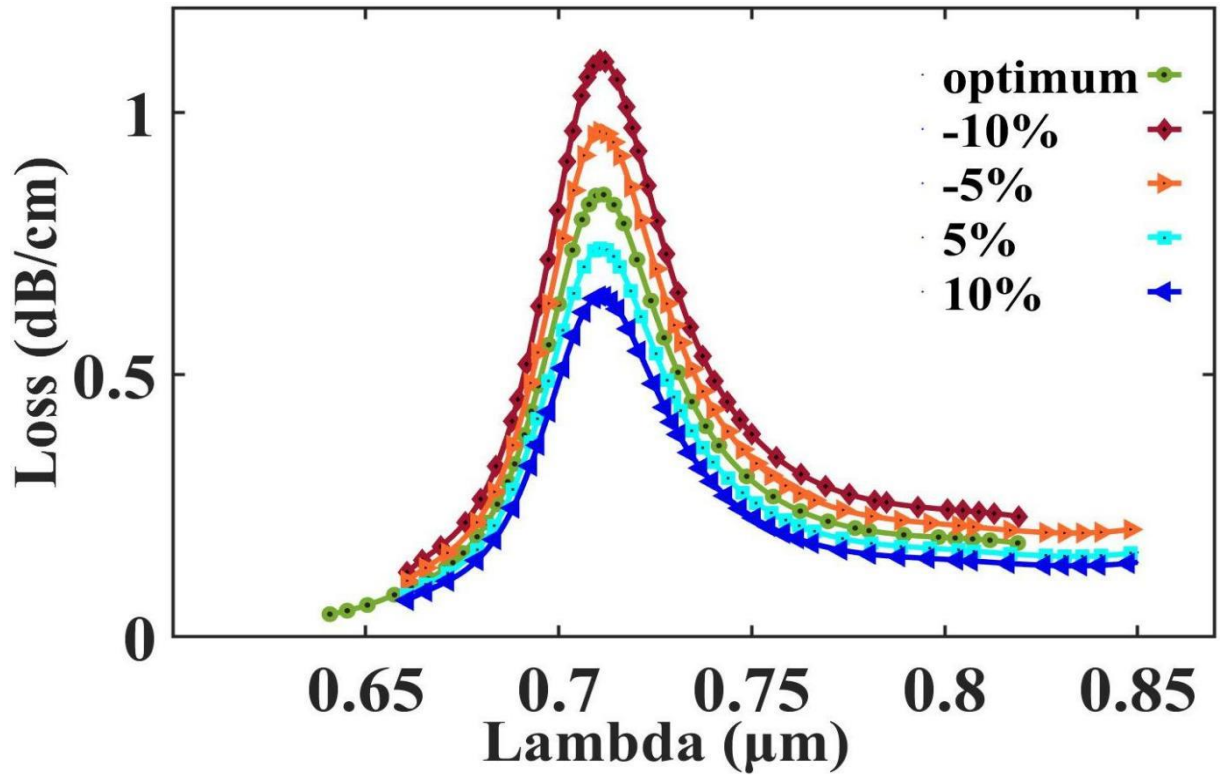
(c)
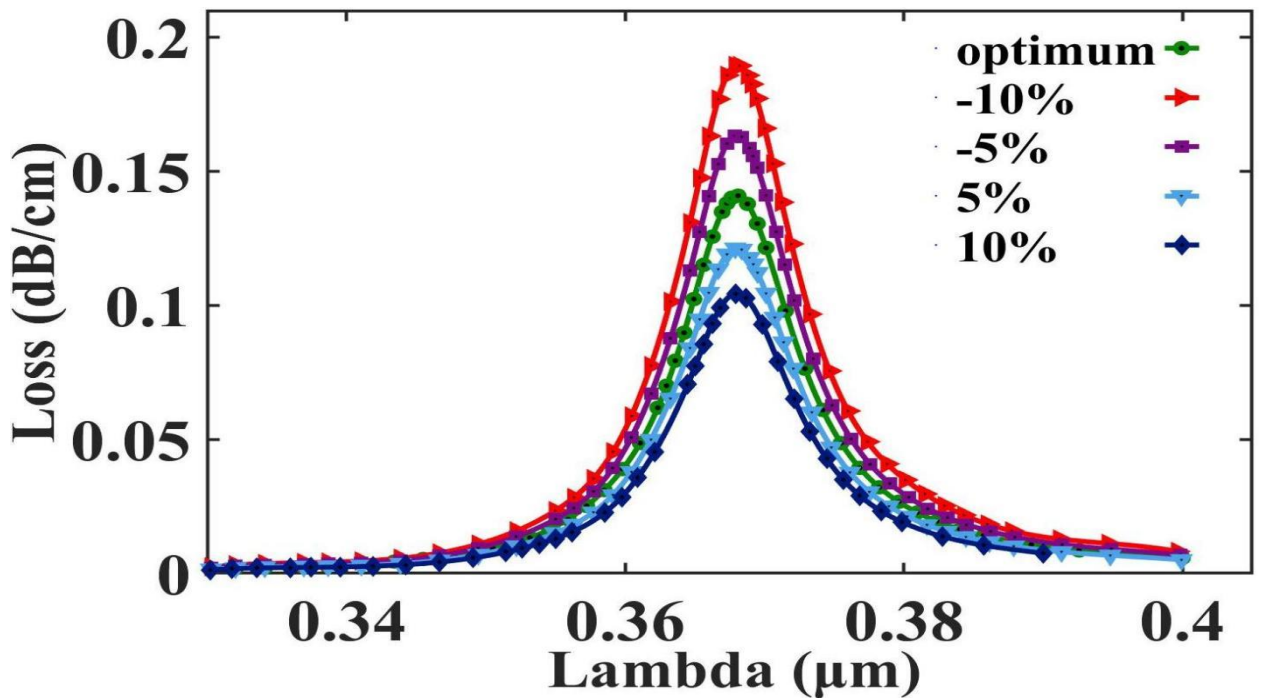
(d)

Fig 14: Loss due to confinement at analyte RI 1.37 with a change of $\pm$5% and $\pm$10% in (a) ITO layer thickness for x-pol (b) ITO layer thickness for y-pol (c) smaller air hole radius for x-pol (d) smaller air hole radius for y-pol

This FT investigation gives support to the resilience and dependability of the PCF SPR sensor design by showing that the sensor's performance maintains within acceptable bounds despite fabrication-related variations. It ensures that even if tiny deviations in the manufacturing process occur, the sensor will continue to work as predicted, closely matching with reported values and attaining accurate detection capabilities.

The design is very useful from the point of view of a new parameter called double polarization peak shift sensitivity (DPPSS) that has wide range of sensing in consideration of both x and y polarizations. The fabrication point of view was also justified with respect to tolerance.

4.6 Comparison

The proposed design shows better performance than many other designs. A list of comparative analysis of the proposed design with other research works in terms of different parameters is given in Table.3.

Table.3. Comparative analysis of different designs and proposed design with respect to resolution and WS by varying analyte RI

Ref	RI Range	Sensor resolution (Wavelength) (RIU)	WS_{max} (nm/RIU)	Double Polarization Peak Shift Sensitivity (DPPSS) (nm/RIU)
[27]	1.33-1.42	5.00×10^{-6}	20,000	---
[28]	1.33–1.39	1.428×10^{-6}	32,000	---
[29]	1.40–1.46	6.25×10^{-6}	16,000	---
[30]	1.33–1.38	2.17×10^{-5}	4600	---
[31]	1.33-1.41	5.88×10^{-6}	17,000	---
[32]	1.33-1.42	7.00×10^{-6}	11,000	---
Proposed design	1.30-1.41	5.09×10^{-6}	19,630	19560

It is therefore observed that the proposed sensor shows a comparatively better result in terms of wavelength sensitivity and resolution. The optimization was done with respect to DPPSS and that is why the Amplitude Sensitivity is comparatively lower. With this, a new sensing parameter has been introduced which takes both the polarizations into consideration. This research is a new dimension for a novel sensing parameter. Achieving better sensitivity in LSPR (Localized Surface Plasmon Resonance) sensors is a crucial objective to enhance their performance and enable the detection of analytes at lower concentrations. LSPR sensors are sensitive to changes in the refractive index of the surrounding medium. Researchers leverage this property by designing LSPR sensors to operate in the proximity of their plasmon resonance wavelength. This ensures that even small changes in the refractive index induced by analyte binding result in significant shifts in the LSPR spectrum, thereby improving sensitivity. LSPR sensors rely on the local electromagnetic field enhancement around plasmonic nanostructures. Researchers explore strategies to maximize this enhancement, such as optimizing the distance between nanoparticles or incorporating nanostructured substrates. These approaches can lead to higher sensitivity by intensifying the interaction between the analyte and the localized surface plasmons.

CHAPTER 5

CONCLUSION AND FUTURE PROSPECTS

5.1 CONCLUSION

In this research, we are presenting a comprehensive study of an LSPR-based sensor with a unique combination of two metals ITO and Au and its performance is analyzed using FEM method. For this, the interaction of leaky core modes with surface plasmons causes resonance, which results in varied responses due to changes in the surrounding medium. Practically, it has been observed that the PCF that was a silica-based glass fiber has low adhesion with the Au layer, which could reduce sensing capability. Ag in a combination of Au might resolve the issue but the RI range stays narrow which limits many practical aspects. Therefore, we are proposing ITO as a plasmonic layer in combination with Au to increase the RI range of 1.30 to 1.40. The proposed sensor design has the maximum double polarization peak shift sensitivity (DPPSS) value of 19560 nm/RIU and maximum WS of 19630 nm/RIU. The AS of the proposed design is low because while optimizing the geometrical parameters, we tried to achieve the maximum DPPSS. The maximum AS value achieved was 646.18 RIU^{-1}.

The tradeoff between Amplitude Sensitivity and DPPSS was chosen in this case. As the new parameter named DPPSS was introduced, steps were taken to achieve maximum sensitivity in terms of DPPSS. As the optimization was not done with respect to amplitude Sensitivity, that is why the AS is comparatively less.

In conclusion, the proposed Localized Surface Plasmon Resonance (LSPR) sensor stands out as the best option for several reasons. Its unique design and functionality offer numerous advantages over alternative sensing technologies, making it highly suitable for a wide range of applications.

Firstly, the LSPR sensor demonstrates exceptional sensitivity and selectivity. Its ability to detect small changes in refractive index or adsorption events at the nanoscale level is unparalleled. This high sensitivity ensures accurate and reliable measurements, even in complex and dynamic environments.

Secondly, the LSPR sensor offers a versatile and flexible platform. Its compatibility with various materials, including metals, dielectrics, and semiconductors, enables customization and optimization to meet specific requirements. This adaptability extends its utility across multiple disciplines, such as biomedical, environmental monitoring, and chemical analysis.

Moreover, the LSPR sensor excels in real-time monitoring. Its label-free detection method eliminates the need for additional chemical or molecular tags, simplifying experimental procedures and reducing costs. This real-time capability allows for continuous and instantaneous analysis, enabling timely decision-making and intervention.

Furthermore, the LSPR sensor boasts a compact and miniaturized design. Its small footprint and low power consumption make it suitable for integration into portable and wearable devices, expanding its potential applications in point-of-care diagnostics and personalized healthcare.

Additionally, the LSPR sensor offers long-term stability and durability. Its robust construction and resistance to environmental factors ensure consistent and reliable performance over extended periods. This reliability translates into reduced maintenance requirements and increases operational efficiency.

Lastly, the LSPR sensor exhibits great potential for further advancements and innovations. Ongoing research and development in nanomaterials, plasmonics, and fabrication techniques continue to enhance its performance, sensitivity, and versatility. The future integration of LSPR sensors with other technologies, such as microfluidics and machine learning, promises even greater capabilities and broader applications.

Overall, the proposed LSPR sensor surpasses its competitors by virtue of its exceptional sensitivity, versatility, real-time monitoring, compact design, long-term stability, and potential for further advancements. Its unique attributes make it the best choice for numerous applications, paving the way for exciting developments in sensing technology and scientific discoveries.

5.2 Future Prospect

With the promising results obtained from this research work, we plan to grow the area of our knowledge and research in different other ways. One of the most important phenomena that comes to our mind in this regard is the integration of machine learning for determining

simulated values of confinement loss and other parameters. As the research work was done keeping randomly chosen value as optimized and then optimizing the other parameters with respect to that, so there always remain a slight inconvenience and discrepancies on whether the order of optimization is right or not. This is the reason why incorporation of Machine learning technology is worthy of being proven beneficial to complete all the simulations at the same time keeping the values optimized to the maximum level. LSPR sensors can be integrated with other emerging technologies to unlock new functionalities and applications. For example, combining LSPR sensors with microfluidics enables the development of lab-on-a-chip devices for rapid and high-throughput analysis. Integration with artificial intelligence and machine learning algorithms could enhance the capabilities of LSPR sensors, allowing for intelligent data analysis, pattern recognition, and improved sensor performance.

On the other hand, it has been observed that the optimization of smaller air holes came down to the value of 1 nm. Although theoretically this is the most optimized value, keeping the practical implementation in mind there is a concern of making the sensor fabrication friendly. Continued advancements in nanomaterials synthesis and fabrication techniques are expected to further enhance the performance of LSPR sensors. Innovations in plasmonic materials, nanostructured surfaces, and fabrication processes will lead to increased sensitivity, improved reproducibility, and scalability of LSPR sensors, making them more accessible for widespread adoption.

In summary, the prospects of LSPR sensors are bright and diverse. Their potential applications span various fields, including biomedicine, environmental monitoring, food safety, pharmaceuticals, energy, and optoelectronics. Further developments in nanomaterials, integration with emerging technologies, and advancements in fabrication techniques will continue to expand the capabilities of LSPR sensors, leading to new discoveries, improved sensing performance, and increased practicality in real-world applications.

Future of Optical Sensor

The future of optical sensors looks promising, with ongoing advancements and emerging technologies driving their development and expanding their applications. Here are some key aspects that may shape the future of optical sensors:

Miniaturization and Integration: There is a growing demand for smaller, portable, and integrated sensing devices. The future of optical sensors involves miniaturizing their components and integrating them with other technologies such as microfluidics, electronics,

and wireless communication. This will enable the development of compact, wearable, and networked optical sensor systems.

Sensing Beyond the Visible Spectrum: Optical sensors traditionally operate in the visible spectrum, but the future will likely see an expansion into other regions of the electromagnetic spectrum. This includes the ultraviolet (UV), infrared (IR), and terahertz (THz) ranges. By utilizing these additional spectral ranges, optical sensors can access new information, detect different analytes, and offer enhanced capabilities for various applications.

Advanced Materials and Nanotechnology: The development of novel materials, such as plasmonic nanomaterials, metamaterials, and two-dimensional materials (e.g., graphene), will revolutionize the performance of optical sensors. These materials possess unique optical properties, such as strong light-matter interactions, enhanced sensitivity, and tunability. Nanofabrication techniques will enable precise control of material structures, leading to highly sensitive and selective optical sensors.

Photonics Integration and Chip-scale Sensing: The integration of multiple optical components and functions onto a single chip, known as photonics integration, holds great potential for optical sensors. By combining light sources, detectors, waveguides, and signal processing elements on a single chip, compact and highly functional optical sensor systems can be realized. This technology enables cost-effective mass production and deployment of optical sensors in various fields.

Smart Sensing and Artificial Intelligence: The future of optical sensors involves incorporating artificial intelligence (AI) algorithms and machine learning techniques to enable smart sensing capabilities. AI can enhance data processing, pattern recognition, and decision-making in optical sensors, enabling real-time analysis, adaptive measurement strategies, and autonomous operation. This will lead to more efficient and intelligent optical sensing systems.

Biomedical and Healthcare Applications: Optical sensors have significant potential in healthcare and biomedical applications. Future developments may include wearable and implantable optical sensors for continuous monitoring of vital signs, non-invasive glucose

monitoring for diabetes management, early detection of diseases, and point-of-care diagnostics. Optical sensors can also contribute to advances in imaging technologies, such as optical coherence tomography (OCT) and fluorescence imaging.

Environmental Monitoring and Sustainability: Optical sensors will continue to play a vital role in environmental monitoring, contributing to sustainability efforts. They can be used for real-time monitoring of air and water quality, detecting pollutants, and assessing environmental impact. Optical sensors will aid in addressing climate change, pollution control, and resource management.

As technology continues to evolve, the future of optical sensors holds immense potential for addressing pressing societal challenges, advancing scientific research, and enabling innovative applications across various domains.

REFERENCE

[1]   M. R. Islam *et al.*, "Design and numerical analysis of a gold-coated photonic crystal fiber based refractive index sensor," *Opt Quantum Electron*, vol. 53, no. 2, Feb. 2021, doi: 10.1007/s11082-021-02748-8.

[2]   "'https://www.news-medical.net/whitepaper/20161004/LSPR-Technology-The-Four-Most-Frequently-Asked-Questions.aspx.'"

[3]   "'[Online]. Available: https://www.affiniteinstruments.com/post/6-advantages-of-surface-plasmon-resonance-technology.'"

[4]   S. Chakma, M. A. Khalek, B. K. Paul, K. Ahmed, M. R. Hasan, and A. N. Bahar, "Gold-coated photonic crystal fiber biosensor based on surface plasmon resonance: Design and analysis," *Sens Biosensing Res*, vol. 18, pp. 7–12, Apr. 2018, doi: 10.1016/j.sbsr.2018.02.003.

[5]   M. Rakibul Islam, A. N. M. Iftekher, M. S. Anzum, M. Rahman, and S. Siraz, "LSPR Based Double Peak Double Plasmonic Layered Bent Core PCF-SPR Sensor for Ultra-Broadband Dual Peak Sensing," *IEEE Sens J*, vol. 22, no. 6, pp. 5628–5635, 2022, doi: 10.1109/JSEN.2022.3149715.

[6]   C. Liu *et al.*, "Surface plasmon resonance (SPR) infrared sensor based on D-shape photonic crystal fibers with ITO coatings," *Opt Commun*, vol. 464, Jun. 2020, doi: 10.1016/j.optcom.2020.125496.

[7]   S. Franzen, "Surface plasmon polaritons and screened plasma absorption in indium tin oxide compared to silver and gold," *Journal of Physical Chemistry C*, vol. 112, no. 15, pp. 6027–6032, Apr. 2008, doi: 10.1021/jp7097813.

[8]   S. A. Zynio, A. V Samoylov, E. R. Surovtseva, V. M. Mirsky, and Y. M. Shirshov, "Bimetallic Layers Increase Sensitivity of Affinity Sensors Based on Surface Plasmon Resonance," *Sensors*, vol. 2, pp. 62–70, 2002, [Online]. Available: http://www.mdpi.net/sensors

[9]   P. A. Sohi and M. Kahrizi, "Principles and Applications of Nanoplasmonics in Biological and Chemical Sensing: A Review," in *Recent Advances in Nanophotonics - Fundamentals and Applications*, IntechOpen, 2020. doi: 10.5772/intechopen.93001.

[10]   A. K. Shakya and S. Singh, "Design and analysis of dual polarized Au and TiO 2-coated photonic crystal fiber surface plasmon resonance refractive index sensor: an extraneous sensing approach," 2021, doi: 10.1117/1.JNP.15.

[11]   P. Sharma and P. Sharan, "Design of photonic crystal based ring resonator for detection of different blood constituents," *Opt Commun*, vol. 348, pp. 19–23, 2015, doi: https://doi.org/10.1016/j.optcom.2015.03.015.

[12]   K. Ahmed *et al.*, "Refractive Index Based Blood Components Sensing in Terahertz Spectrum."

[13] M. R. Islam, A. N. M. Iftekher, F. A. Mou, M. M. Rahman, and M. I. H. Bhuiyan, "Design of a Topas-based ultrahigh-sensitive PCF biosensor for blood component detection," *Appl Phys A Mater Sci Process*, vol. 127, no. 2, Feb. 2021, doi: 10.1007/s00339-020-04261-3.

[14] M. M. Rahman, F. A. Mou, M. I. H. Bhuiyan, and M. R. Islam, "Photonic crystal fiber based terahertz sensor for cholesterol detection in human blood and liquid foodstuffs," *Sens Biosensing Res*, vol. 29, Aug. 2020, doi: 10.1016/j.sbsr.2020.100356.

[15] M. R. Islam, M. A. Hossain, K. M. A. Talha, and R. K. Munia, "A novel hollow core photonic sensor for liquid analyte detection in the terahertz spectrum: design and analysis," *Opt Quantum Electron*, vol. 52, no. 9, Sep. 2020, doi: 10.1007/s11082-020-02532-0.

[16] M. A. Islam, M. R. Islam, A. M. Al Naser, F. Anzum, and F. Z. Jaba, "Square structured photonic crystal fiber based THz sensor design for human body protein detection," *J Comput Electron*, vol. 20, no. 1, pp. 377–386, Feb. 2021, doi: 10.1007/s10825-020-01606-2.

[17] M. R. Islam *et al.*, "Surface plasmon resonance based highly sensitive gold coated PCF biosensor," *Appl Phys A Mater Sci Process*, vol. 127, no. 2, Feb. 2021, doi: 10.1007/s00339-020-04162-5.

[18] M. R. Islam *et al.*, "Design and numerical analysis of a gold-coated photonic crystal fiber based refractive index sensor," *Opt Quantum Electron*, vol. 53, no. 2, Feb. 2021, doi: 10.1007/s11082-021-02748-8.

[19] M. A. Islam, M. R. Islam, S. Siraz, M. Rahman, M. S. Anzum, and F. Noor, "Wheel structured Zeonex-based photonic crystal fiber sensor in THz regime for sensing milk," *Appl Phys A Mater Sci Process*, vol. 127, no. 5, May 2021, doi: 10.1007/s00339-021-04472-2.

[20] M. R. Islam, A. N. M. Iftekher, F. Noor, M. R. H. Khan, M. T. Reza, and M. M. Nishat, "AZO-coated plasmonic PCF nanosensor for blood constituent detection in near-infrared and visible spectrum," *Appl Phys A Mater Sci Process*, vol. 128, no. 1, Jan. 2022, doi: 10.1007/s00339-021-05220-2.

[21] M. R. Islam *et al.*, "An Eye-Shaped Ultra-Sensitive Localized Surface Plasmon Resonance–Based Biochemical Sensor," *Plasmonics*, vol. 17, no. 1, pp. 131–141, Feb. 2022, doi: 10.1007/s11468-021-01501-x.

[22] M. R. Islam *et al.*, "Design of a Dual Cluster and Dual Array-Based PCF-SPR Biosensor with Ultra-high WS and FOM," *Plasmonics*, vol. 17, no. 3, pp. 1171–1182, Jun. 2022, doi: 10.1007/s11468-022-01612-z.

[23] M. M. Rahman, F. A. Mou, M. I. H. Bhuiyan, M. A. Al Mahmud, and M. R. Islam, "Design and characterization of a photonic crystal fiber for improved THz wave propagation and analytes sensing," *Opt Quantum Electron*, vol. 54, no. 10, Oct. 2022, doi: 10.1007/s11082-022-04057-0.

[24] M. R. Islam *et al.*, "Design of a quad channel SPR-based PCF sensor for analyte, strain, temperature, and magnetic field strength sensing," *Opt Quantum Electron*, vol. 54, no. 9, Sep. 2022, doi: 10.1007/s11082-022-03912-4.

[25]   M. R. Islam, T. T. Treena, N. M. Munim, and S. I. Ali, "Peak amplitude difference sensitivity (PADS): An interrogation technique for PCF-SPR sensors using symmetrical arrays of plasmonic layers," *Results Phys*, vol. 48, May 2023, doi: 10.1016/j.rinp.2023.106434.

[26]   M. R. Islam *et al.*, "Design and analysis of birefringent SPR based PCF biosensor with ultra-high sensitivity and low loss," *Optik (Stuttg)*, vol. 221, Nov. 2020, doi: 10.1016/j.ijleo.2020.165311.

[27]   M. R. Islam *et al.*, "Trigonal cluster-based ultra-sensitive surface plasmon resonance sensor for multipurpose sensing," *Sens Biosensing Res*, vol. 35, Feb. 2022, doi: 10.1016/j.sbsr.2022.100477.

[28]   B. Liedberg, C. Nylander, and I. Lunström, "Surface plasmon resonance for gas detection and biosensing," *Sensors and Actuators*, vol. 4, pp. 299–304, 1983, doi: https://doi.org/10.1016/0250-6874(83)85036-7.

[29]   M. Rakibul Islam, M. M. I. Khan, F. Mehjabin, J. Alam Chowdhury, and M. Islam, "Design of a fabrication friendly & highly sensitive surface plasmon resonance-based photonic crystal fiber biosensor," *Results Phys*, vol. 19, Dec. 2020, doi: 10.1016/j.rinp.2020.103501.

[30]   M. R. Islam *et al.*, "Design and Analysis of a Biochemical Sensor Based on Surface Plasmon Resonance with Ultra-high Sensitivity," *Plasmonics*, vol. 16, no. 3, pp. 849–861, Jun. 2021, doi: 10.1007/s11468-020-01355-9.

[31]   R. K. Verma and B. D. Gupta, "Surface plasmon resonance based fiber optic sensor for the IR region using a conducting metal oxide film," 2010.

[32]   S. W. James and R. P. Tatam, "Optical fibre long-period grating sensors: Characteristics and application," *Meas Sci Technol*, vol. 14, no. 5, 2003, doi: 10.1088/0957-0233/14/5/201.

[33]   A. K. Sharma, R. Jha, and B. D. Gupta, "Fiber-Optic Sensors Based on Surface Plasmon Resonance: A Comprehensive Review," *IEEE Sens J*, vol. 7, pp. 1118–1129, 2007.

[34]   Md. S. Islam *et al.*, "A novel Zeonex based photonic sensor for alcohol detection in beverages," in *2017 IEEE International Conference on Telecommunications and Photonics (ICTP)*, 2017, pp. 114–118. doi: 10.1109/ICTP.2017.8285905.

[35]   M. M. Rahman, F. A. Mou, M. I. H. Bhuiyan, and M. R. Islam, "Photonic crystal fiber based terahertz sensor for cholesterol detection in human blood and liquid foodstuffs," *Sens Biosensing Res*, vol. 29, Aug. 2020, doi: 10.1016/j.sbsr.2020.100356.

[36]   M. R. Islam *et al.*, "Design of a Dual Cluster and Dual Array-Based PCF-SPR Biosensor with Ultra-high WS and FOM," *Plasmonics*, vol. 17, no. 3, pp. 1171–1182, Jun. 2022, doi: 10.1007/s11468-022-01612-z.

[37]   C. Mouvet *et al.*, "Determination of simazine in water samples by waveguide surface plasmon resonance," *Anal Chim Acta*, vol. 338, no. 1, pp. 109–117, 1997, doi: https://doi.org/10.1016/S0003-2670(96)00443-6.

[38]   B. Han *et al.*, "Simultaneous measurement of temperature and strain based on dual SPR effect in PCF," *Opt Laser Technol*, vol. 113, pp. 46–51, May 2019, doi: 10.1016/j.optlastec.2018.12.010.

[39]   L. Rindorf, J. B. Jensen, M. Dufva, L. H. Pedersen, P. E. Høiby, and O. Bang, "Photonic crystal fiber long-period gratings for biochemical sensing," *Opt. Express*, vol. 14, no. 18, pp. 8224–8231, Sep. 2006, doi: 10.1364/OE.14.008224.

[40]   S. Weng, L. Pei, J. Wang, T. Ning, and J. Li, "High sensitivity D-shaped hole fiber temperature sensor based on surface plasmon resonance with liquid filling," *Photon. Res.*, vol. 5, no. 2, pp. 103–107, Apr. 2017, doi: 10.1364/PRJ.5.000103.

[41]   J.-K. Wang, K. Xu, and G.-Y. Si, "High sensitivity D-shaped optical fiber strain sensor based on surface plasmon resonance," *Opt Commun*, vol. 460, p. 125147, May 2019, doi: 10.1016/j.optcom.2019.125147.

[42]   S. Chakma, M. A. Khalek, B. K. Paul, K. Ahmed, M. R. Hasan, and A. N. Bahar, "Gold-coated photonic crystal fiber biosensor based on surface plasmon resonance: Design and analysis," *Sens Biosensing Res*, vol. 18, pp. 7–12, 2018, doi: https://doi.org/10.1016/j.sbsr.2018.02.003.

[43]   A. A. Rifat *et al.*, "Photonic crystal fiber based plasmonic sensors," *Sensors and Actuators, B: Chemical*, vol. 243. Elsevier B.V., pp. 311–325, May 01, 2017. doi: 10.1016/j.snb.2016.11.113.

[44]   M. A. Mollah, S. M. R. Islam, M. Yousufali, L. F. Abdulrazak, M. B. Hossain, and I. S. Amiri, "Plasmonic temperature sensor using D-shaped photonic crystal fiber," *Results Phys*, vol. 16, Mar. 2020, doi: 10.1016/j.rinp.2020.102966.

[45]   D. Krohn, "Fiber Optic Sensors: Fundamentals and Applications," 2015.

[46]   F. (Federica) Poli, A. (Annamaria) Cucinotta, and Stefano. Selleri, *Photonic crystal fibers : properties and applications*. Springer, 2007.

[47]   J. Sultana, Md. S. Islam, K. Ahmed, A. Dinovitser, B. W.-H. Ng, and D. Abbott, "Terahertz detection of alcohol using a photonic crystal fiber sensor," *Appl. Opt.*, vol. 57, no. 10, pp. 2426–2433, Apr. 2018, doi: 10.1364/AO.57.002426.

[48]   Y. Zhao, R. Tong, F. Xia, and Y. Peng, "Current status of optical fiber biosensor based on surface plasmon resonance," *Biosens Bioelectron*, vol. 142, p. 111505, 2019, doi: https://doi.org/10.1016/j.bios.2019.111505.

[49]   Y. Zhao, X. Hu, S. Hu, and Y. Peng, "Applications of fiber-optic biochemical sensor in microfluidic chips: A review," *Biosens Bioelectron*, vol. 166, p. 112447, 2020, doi: https://doi.org/10.1016/j.bios.2020.112447.

[50]   S. W. James and R. P. Tatam, "Optical fibre long-period grating sensors: Characteristics and application," *Meas Sci Technol*, vol. 14, no. 5, 2003, doi: 10.1088/0957-0233/14/5/201.

[51] Md. S. Islam, M. R. Islam, J. Sultana, A. Dinovitser, B. W.-H. Ng, and D. Abbott, "Exposed-core localized surface plasmon resonance biosensor," *Journal of the Optical Society of America B*, vol. 36, no. 8, p. 2306, Aug. 2019, doi: 10.1364/josab.36.002306.

[52] M. Islam *et al.*, "A Novel Approach for Spectroscopic Chemical Identification Using Photonic Crystal Fiber in the Terahertz Regime," *IEEE Sens J*, vol. 18, pp. 575–582, May 2018, doi: 10.1109/JSEN.2017.2775642.

[53] B. Liedberg, C. Nylander, and I. Lunström, "Surface plasmon resonance for gas detection and biosensing," *Sensors and Actuators*, vol. 4, pp. 299–304, 1983, doi: https://doi.org/10.1016/0250-6874(83)85036-7.

[54] E. K. Akowuah, T. Gorman, H. Ademgil, S. Haxha, G. K. Robinson, and J. V Oliver, "Numerical Analysis of a Photonic Crystal Fiber for Biosensing Applications," *IEEE J Quantum Electron*, vol. 48, no. 11, pp. 1403–1410, 2012, doi: 10.1109/JQE.2012.2213803.

[55] B. D. Gupta and R. K. Verma, "Surface Plasmon Resonance-Based Fiber Optic Sensors: Principle, Probe Designs, and Some Applications," *J Sens*, vol. 2009, p. 979761, 2009, doi: 10.1155/2009/979761.

[56] A. A. Rifat *et al.*, "Photonic crystal fiber based plasmonic sensors," *Sens Actuators B Chem*, vol. 243, pp. 311–325, 2017, doi: https://doi.org/10.1016/j.snb.2016.11.113.

[57] J. G. Ortega-Mendoza, A. Padilla-Vivanco, C. Toxqui-Quitl, P. Zaca-Morán, D. Villegas-Hernández, and F. Chávez, "Optical Fiber Sensor Based on Localized Surface Plasmon Resonance Using Silver Nanoparticles Photodeposited on the Optical Fiber End," *Sensors*, vol. 14, no. 10, pp. 18701–18710, 2014, doi: 10.3390/s141018701.

[58] J. Homola, "Present and future of surface plasmon resonance biosensors," *Anal Bioanal Chem*, vol. 377, no. 3, pp. 528–539, 2003, doi: 10.1007/s00216-003-2101-0.

[59] R. Otupiri, E. K. Akowuah, S. Haxha, H. Ademgil, F. AbdelMalek, and A. Aggoun, "A Novel Birefrigent Photonic Crystal Fiber Surface Plasmon Resonance Biosensor," *IEEE Photonics J*, vol. 6, no. 4, pp. 1–11, 2014, doi: 10.1109/JPHOT.2014.2335716.

[60] M. R. Islam *et al.*, "Design of a dual spider-shaped surface plasmon resonance-based refractometric sensor with high amplitude sensitivity," *IET Optoelectronics*, vol. 17, no. 1, pp. 38–49, 2023, doi: https://doi.org/10.1049/ote2.12084.

[61] M. R. Islam, E. Moazzam, R. Islam, R. L. Khan, and Z. Tasnim, "Design and Investigation of a low-loss Surface Plasmon resonance based PCF biosensor with a gold coated structure," in *Proceedings of 2020 11th International Conference on Electrical and Computer Engineering, ICECE 2020*, Institute of Electrical and Electronics Engineers Inc., Dec. 2020, pp. 447–450. doi: 10.1109/ICECE51571.2020.9393045.

[62] F. A. Mou, Md. M. Rahman, M. R. Islam, and M. I. H. Bhuiyan, "Development of a photonic crystal fiber for THz wave guidance and environmental pollutants detection," *Sens Biosensing Res*, vol. 29, p. 100346, 2020, doi: https://doi.org/10.1016/j.sbsr.2020.100346.

[63]   M. R. Islam *et al.*, "Highly birefringent gold-coated SPR sensor with extremely enhanced amplitude and wavelength sensitivity," *Eur Phys J Plus*, vol. 136, no. 2, Feb. 2021, doi: 10.1140/epjp/s13360-021-01220-6.

[64]   S. A. Maier, "Plasmonics: The Promise of Highly Integrated Optical Devices," *IEEE Journal of Selected Topics in Quantum Electronics*, vol. 12, no. 6, pp. 1671–1677, 2006, doi: 10.1109/JSTQE.2006.884086.

[65]   S. P. Burgos, H. W. Lee, E. Feigenbaum, R. M. Briggs, and H. A. Atwater, "Synthesis and Characterization of Plasmonic Resonant Guided Wave Networks," *Nano Lett*, vol. 14, no. 6, pp. 3284–3292, Jun. 2014, doi: 10.1021/nl500694c.

[66]   M. A. Al Mahmud, M. R. Islam, A. N. M. Iftekher, M. M. Rahman, and F. A. Mou, "Design and numerical analysis of a porous core photonic crystal fiber for refractometric THz sensing," *Microsystem Technologies*, vol. 29, no. 1, pp. 115–126, Jan. 2023, doi: 10.1007/s00542-022-05396-4.

[67]   M. R. Islam, Md. F. Kabir, K. Md. A. Talha, and Md. S. Islam, "A novel hollow core terahertz refractometric sensor," *Sens Biosensing Res*, vol. 25, p. 100295, 2019, doi: https://doi.org/10.1016/j.sbsr.2019.100295.

[68]   M. Islam, J. Sultana, R. A. Aoni, A. Dinovitser, B. Ng, and D. Abbott, "Terahertz Sensing in a Hollow Core Photonic Crystal Fiber," *IEEE Sens J*, vol. 18, pp. 4073–4080, May 2018, doi: 10.1109/JSEN.2018.2819165.

[69]   S. Al Tahhan and H. Aljobouri, "Sensing of Illegal Drugs by Using Photonic Crystal Fiber in Terahertz Regime," *Journal of Optical Communications*, vol. 1, May 2020, doi: 10.1515/joc-2019-0291.

[70]   J. Wu, S. Li, X. Wang, M. Shi, X. Feng, and Y. Liu, "Ultrahigh sensitivity refractive index sensor of a D-shaped PCF based on surface plasmon resonance," *Appl. Opt.*, vol. 57, no. 15, pp. 4002–4007, May 2018, doi: 10.1364/AO.57.004002.

[71]   Md. Ibadul Islam *et al.*, "Design of single mode spiral photonic crystal fiber for gas sensing applications," *Sens Biosensing Res*, vol. 13, pp. 55–62, 2017, doi: https://doi.org/10.1016/j.sbsr.2017.03.001.

[72]   K. Ahmed, M. Morshed, S. Asaduzzaman, and Md. F. H. Arif, "Optimization and enhancement of liquid analyte sensing performance based on square-cored octagonal photonic crystal fiber," *Optik - International Journal for Light and Electron Optics*, vol. 131, pp. 687–696, May 2017, doi: 10.1016/j.ijleo.2016.11.171.

[73]   M. Islam, F. Mou, Md. M. Rahman, and M. Bhuiyan, "Hollow Core Photonic Crystal Fiber for Chemicals sensing in Liquid Analytes," *Int J Mod Phys B*, vol. 34, May 2020, doi: 10.1142/S0217979220502598.

[74]   A. Ramachandran, P. R. Babu, and K. Senthilnathan, "Sensitivity analysis of steering-wheel gas sensor against diverse core air hole sizes and core materials in terahertz wave band," *IOP Conf Ser Mater Sci Eng*, vol. 263, 2017.

[75]   M. M. Rahman, F. A. Mou, M. I. H. Bhuiyan, and M. R. Islam, "Refractometric THz Sensing of Blood Components in a Photonic Crystal Fiber Platform," *Brazilian Journal of Physics*, vol. 52, no. 2, Apr. 2022, doi: 10.1007/s13538-022-01054-2.

[76]   M. R. Islam and M. Mamadou, "Spider web ultrasensitive terahertz photonic crystal fiber for chemical sensing," *Optical Engineering*, vol. 59, no. 08, Aug. 2020, doi: 10.1117/1.oe.59.8.087103.

[77]   M. S. Islam *et al.*, "A Hi-Bi Ultra-Sensitive Surface Plasmon Resonance Fiber Sensor," *IEEE Access*, vol. 7, pp. 79085–79094, 2019, doi: 10.1109/ACCESS.2019.2922663.

[78]   V. Kaur and S. Singh, "Design of titanium nitride coated PCF-SPR sensor for liquid sensing applications," *Optical Fiber Technology*, vol. 48, pp. 159–164, Mar. 2019, doi: 10.1016/j.yofte.2018.12.015.

[79]   C. Rhodes *et al.*, "Dependence of plasmon polaritons on the thickness of indium tin oxide thin films," *J Appl Phys*, vol. 103, no. 9, 2008, doi: 10.1063/1.2908862.

[80]   R. W. Gerber, D. N. Leonard, and S. Franzen, "Conductive thin film multilayers of gold on glass formed by self-assembly of multiple size gold nanoparticles," *Thin Solid Films*, vol. 517, no. 24, pp. 6803–6808, Oct. 2009, doi: 10.1016/j.tsf.2009.05.033.

[81]   K. L. Kelly, E. Coronado, L. L. Zhao, and G. C. Schatz, "The optical properties of metal nanoparticles: The influence of size, shape, and dielectric environment," *Journal of Physical Chemistry B*, vol. 107, no. 3, pp. 668–677, Jan. 2003, doi: 10.1021/jp026731y.

[82]   L. Wang, M. Hasanzadeh Kafshgari, and M. Meunier, "Optical Properties and Applications of Plasmonic-Metal Nanoparticles," *Advanced Functional Materials*, vol. 30, no. 51. Wiley-VCH Verlag, Dec. 01, 2020. doi: 10.1002/adfm.202005400.

[83]   J.-C. Kim, H.-K. Kim, U.-C. Paek, B.-H. Lee, and J.-B. Eom, "The Fabrication of a Photonic Crystal Fiber and Measurement of its Properties," *J Opt Soc Korea*, vol. 7, no. 2, pp. 79–83, Jun. 2003, doi: 10.3807/josk.2003.7.2.079.

[84]   M. R. Islam *et al.*, "Design and numerical analysis of a gold-coated photonic crystal fiber based refractive index sensor," *Opt Quantum Electron*, vol. 53, no. 2, Feb. 2021, doi: 10.1007/s11082-021-02748-8.